



저작자표시-비영리-변경금지 2.0 대한민국

이용자는 아래의 조건을 따르는 경우에 한하여 자유롭게

- 이 저작물을 복제, 배포, 전송, 전시, 공연 및 방송할 수 있습니다.

다음과 같은 조건을 따라야 합니다:



저작자표시. 귀하는 원저작자를 표시하여야 합니다.



비영리. 귀하는 이 저작물을 영리 목적으로 이용할 수 없습니다.



변경금지. 귀하는 이 저작물을 개작, 변형 또는 가공할 수 없습니다.

- 귀하는, 이 저작물의 재이용이나 배포의 경우, 이 저작물에 적용된 이용허락조건을 명확하게 나타내어야 합니다.
- 저작권자로부터 별도의 허가를 받으면 이러한 조건들은 적용되지 않습니다.

저작권법에 따른 이용자의 권리는 위의 내용에 의하여 영향을 받지 않습니다.

이것은 [이용허락규약\(Legal Code\)](#)을 이해하기 쉽게 요약한 것입니다.

[Disclaimer](#)

교육학석사 학위논문

Identification of Cyclophilin Inhibitors Using One-Bead-One-Compound Cyclic Peptoid Library

One-Bead-One-Compound 고리형 펩토이드
라이브러리를 이용한 사이클로필린 저해제 발굴

2021 년 2 월

서울대학교 대학원
과학교육과 화학전공
박 남 준

Identification of Cyclophilin Inhibitors using One-bead-one-compound Cyclic Peptoid Library

지도 교수 유재훈

이 논문을 교육학석사 학위논문으로 제출함

2020 년 12 월

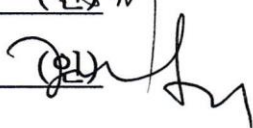
서울대학교 대학원

과학교육과 화학전공

박 남 준

박남준의 교육학석사 학위논문을 인준함

2021 년 2 월

위원장 장대홍 (인) 
부위원장 유재훈 (인) 
위원 YU JUNHUA (인) 

Abstract

Identification of Cyclophilin Inhibitors Using One-Bead-One-Compound Cyclic Peptoid Library

Namjoon Park

Department of Science Education

(Major in Chemistry)

The Graduate School

Seoul National University

Cyclophilins (Cyps) are peptidyl-prolyl isomerases (PPIases) which catalyze cis-trans isomerization of peptidyl-proline. Among 17 human Cyp isoforms, first identified and most abundant isoform, cyclophilin A is mainly expressed in cytosol, involved in several human diseases such as rheumatoid arthritis (RA), Alzheimer's

disease (AD), cancer and viral infection. Another important therapeutic target isoform, cyclophilin D (CypD) is located in mitochondrial matrix, known as a key player of Ca^{2+} induced opening of mitochondrial permeability transition pore (mPTP). Opening of mPTP causes the loss of mitochondrial inner membrane potential, releasing cytochrome c to cytosol, which leads to mitochondria-driven apoptosis. The well-known natural Cyp binder, cyclosporine A (CsA) inhibits the activities of the Cyps at low concentrations. However, the limited use of CsA owing to its undruggable properties such as high cytotoxicity, low solubility and poor BBB permeability suggests the necessity of new strategies or even new compounds that can replace CsA. Herein, One-bead-one-compound (OBOC) cyclic peptoid library was used for the identification of de novo cyclophilin inhibitors. Ten selected compounds were individually synthesized and their inhibitory activities against Cyps were monitored. Compared to CsA, cyclic peptoid I11 showed equipotent inhibition of CypD activity with lower cytotoxicity and better BBB permeability.

Keyword: cyclophilin A, cyclophilin D, one-bead-one-compound, library screening, peptoid, peptidomimetic, mitochondrial permeability transition pore, blood-brain barrier

Student Number: 2018-22030

Contents

Abstract	i
Contents	iii
List of tables	v
List of figures	v
Introduction	1
Experimental Section	4
1. Peptoid synthesis	4
1.1 Synthesis of cyclic peptoids	
1.2 Synthesis of TAMRA-labeled cyclic peptoids	
1.3 Synthesis of Cy5.5-labeled I11	
2. Anti-inflammatory activity (Real-time PCR)	7
3. Binding affinity measurement	8
3.1 Surface Plasmon Resonance (SPR)	
3.2 Fluorescence Anisotropy	
4. Blood-brain barrier permeability measurement (BBB-PAMPA).....	10
5. Mitochondrial membrane potential recovery (JC-1)	10
5.1 Microplate reader	
5.2 Confocal Laser Scanning Microscopy (CLSM)	
6. Cell viability assay (WST-1)	11
7. Biodistribution	12

Results and Discussion	13
1. Design and Synthesis of macrocyclic peptoid library	13
2. Library screening and selection	14
3. Anti-inflammatory activity	29
4. Binding affinity to CypA	32
5. Optimization of I11	41
6. Binding affinity to CypD	45
7. Blood-brain barrier permeability	47
8. Mitochondrial membrane potential recovery effect	49
9. Cytotoxicity	51
10. Biodistribution	52
Conclusions	54
References	55
Abstract (in Korean)	62

List of tables

Table 1. Names and sequences of 100 peptoids	20
Table 2. Sequence and mass data of cyclic peptoids	28
Table 3. Sequence and mass data of TAMRA-labeled peptoids	39
Table 4. Binding affinity to CypA measured by fluorescence anisotropy	40
Table 5. Binding affinity to CypD measured by fluorescence anisotropy	46
Table 6. Effective permeability (P_e) value from BBB-PAMPA	48
Table 7. Sequence and mass data of Cy5.5-I11	52

List of figures

Figure 1. OBOC cyclic peptoid library construction and screening of CypA inhibitors	16
Figure 2. Amine monomers for peptoid library construction	17
Figure 3. General scheme for the construction of sequenceable OBOC cyclic peptoid library using bi-functional resin.....	18
Figure 4. Synthetic details for the construction of sequenceable OBOC cyclic peptoid library using bi-functional resin	19
Figure 5. Sequences and structures of 10 selected peptoids	21

Figure 6. Synthetic scheme for cyclic peptoids	22
Figure 7. Synthetic details for cyclic peptoids	23
Figure 8. Chromatograms of cyclic peptoids	24
Figure 9. Schematic model for the inhibition of anti-inflammatory activity of CypA by CsA or cyclic peptoids	30
Figure 10. Relative IL-2 inhibition of selected cyclic peptoids	30
Figure 11. Relative IL-2 inhibition of I11	31
Figure 12. Concept of SPR-based relative binding affinity screening	33
Figure 13. Representative SPR sensorgrams for the interaction of selected peptoids with CypA	33
Figure 14. Relative binding affinity of cyclic peptoids	34
Figure 15. Correlation of binding affinity and IL-2 inhibition	34
Figure 16. Synthetic details for TAMRA-labeled cyclic peptoids	35
Figure 17. Chromatograms of TAMRA-labeled cyclic peptoids	37
Figure 18. Fluorescence anisotropy binding curves for CsA-CypA and I11-CypA interaction	40
Figure 19. Glycine scanning of peptoid I11	42
Figure 20. IL-2 inhibition of glycine scanning mutants of I11	42
Figure 21. Modification of peptoid I11	43
Figure 22. Loss of IL-2 inhibition of Npip-to-Nleu substitution of I11	43
Figure 23. Improved IL-2 inhibition of modified I11	44
Figure 24. Fluorescence anisotropy binding curves for CsA-CypD and I11-CypD interaction	46

Figure 25. Concept of BBB-PAMPA	48
Figure 26. Analysis of mitochondrial membrane potential	50
Figure 27. Monitoring of mitochondrial membrane potential using CLSM	50
Figure 28. Effects of CsA and peptoids on viability of SH-SY5Y cells	51
Figure 29. Chromatogram of Cy5.5-I11	52
Figure 30. Biodistribution of Cy5.5-I11	53

Introduction

Cyclophilins (Cyps) are peptidyl-prolyl isomerases (PPIases) which catalyze cis-trans isomerization of peptidyl-proline.¹ These proteins are involved in many human diseases such as Alzheimer's disease, Rheumatoid Arthritis, cancer or viral diseases.²⁻⁶ Human Cyps have 17 isoforms with high sequence similarity but distinct functions and distribution, making them to be involved with various pathologies.⁷

First identified and most abundant isoform,⁸ cyclophilin A (CypA) is mainly located in cytosol and also known to be secreted to extracellular space.⁹⁻¹² The well-known natural product inhibitor of Cyps, cyclosporine A (CsA) binds to CypA, preventing calcineurin, a calcium-induced serine-threonine phosphatase, from activating nuclear factor of activated T cell (NFAT), a transcription factor for immune responses such as production of pro-inflammatory cytokine interleukin 2 (IL-2).^{13, 14}

Another promising therapeutic target isoform, cyclophilin D (CypD) is located in mitochondrial matrix, playing a decisive role in Ca^{2+} induced mitochondrial permeability transition pore (mPTP) opening.¹⁵⁻¹⁷ The opening of mPTP causes the loss of mitochondrial inner membrane potential, releasing cytochrome c to cytosol, which leads to mitochondria-driven apoptosis.¹⁸ CypD-deficiency showed neuronal or mitochondrial protective effect in Traumatic Brain Injury (TBI) and neurodegenerative diseases such as Alzheimer's disease.¹⁹⁻²¹

As a tight binder of Cyps, CsA is utilized as an inhibitor of either CypA or CypD in many studies. In the past, CsA was widely used as an immunosuppressant to

prevent organ transplant rejection.²² CypA-deficient mice showed resistance to CsA-induced immunosuppression,²³ which means the immunosuppressive effect of CsA is mainly from its binding to CypA among several CsA-binding Cyps.

The use of CsA as a drug is limited owing to its properties. The powerful immunosuppressive activity of CsA, in some cases, prevents its use for other non-immunosuppressive purposes. Furthermore, clinical use of CsA showed severe adverse effects, particularly nephrotoxicity.^{24,25} Drugs targeting central nerve system (CNS) diseases require the ability to permeate blood-brain barrier (BBB), the gatekeeper of the CNS.²⁶ However, CsA has poor BBB permeability due to its large molecular volume and the activity of drug efflux pump, P-glycoprotein.^{27,28}

Thereby, a variety of strategies were introduced according to their goals. There have been bunch of studies to overcome the adverse effects and limitations of CsA, many of which were focused on the modification of CsA by the synthesis of its derivatives.²⁹⁻³¹ In other studies, CsA was conjugated with lipophilic cations such as triphenylphosphonium (TPP) or quinolinium to target mitochondria for the selective inhibition of CypD.³²⁻³⁴ De novo identification studies of Cyp inhibitors were also performed with several different strategies such as fragmentation-based methods^{35,36} or virtual screening approach.^{37,38}

Peptoids, a class of peptidomimetic constituted of N-substituted glycines, generally possess better proteolytic stability and cell permeability compared to their peptide counterparts with the same functionalities.³⁹⁻⁴¹ Particularly, cyclic forms are known to have even better cell permeability and more rigid structure which enables tighter

binding to their targets.⁴²

To my knowledge, there has been no study identifying novel inhibitors of Cyps by OBOC (One-Bead-One-Compound) peptoid library screening approach. Herein, therefore, OBOC cyclic peptoid library was constructed to identify the inhibitors of the most important therapeutic target isoforms, CypA and CypD. As Cyps have highly conserved sequence among the isoforms, especially in their binding pockets, the representative CypA was used to screen Cyp inhibitors. From the MS/MS sequencing data, ten compounds were synthesized and their potency as Cyp inhibitors were evaluated. Compared to CsA, peptoid I11 showed equipotent inhibition of CypD activity, represented as mitochondrial membrane potential recovery effect, with better BBB permeability and lower cytotoxicity.

Experimental Section

1. Peptoid synthesis

1.1 Synthesis of cyclic peptoids

Rink amide MBHA resins (100 mg, 0.051 mmol, 0.51 mmol/g) were swollen with dimethylformamide (DMF, 5 mL, RT, 5 min). The resins were placed in a microwave vessel with 5 mL of 20% piperidine in DMF and irradiated for 2 min (ramping time for 1 min) at 5 W power on an SPSS microwave peptide synthesizer (Discover, CEM). The resins were washed with DMF (5 mL \times 1 min, 3 times) and dichloromethane (DCM, 5 mL \times 1 min, 3 times). Then, a solution of *N*- α -Fmoc-Cys(4-methoxytrityl)-OH (63 mg, 0.10 mmol), Benzotriazole-1-yl-oxy-tris-pyrrolidino-phosphonium hexafluorophosphate (PyBOP, 53 mg, 0.10 mmol) and *N,N*-diisopropylethylamine (DIPEA, 17.8 μ L, 0.10 mmol) in 5 mL of DMF were added and microwave irradiated for 5 min (ramping time for 2 min) at 5 W power. The temperature was set at 35 °C for both Fmoc deprotection and coupling step.

For peptoid coupling, amidation with bromoacetic acid (BAA) and S_N2 substitution reaction by various primary amines were performed in sequence. Briefly, the primary amines were then performed amidation reaction with bromoacetic acid (BAA) (2 M in DMF, 1.0 mmol, 20 eq) and diisopropylcarbodiimide (DIC) (2 M in DMF, 1.0 mmol, 20 eq) by microwave irradiation at 35 °C for 2 minutes 2 min. After the washing step, Br was substituted with an amine (2 M in DMF, 1.0 mmol, 20 eq) at RT for 2 h. This bromoacetylation-amination cycle was repeated overall 5 times

to complete the sequence of each penta-peptoid. When the fifth amination was completed, the beads were treated with chloroacetic anhydride (CAA) (2 M in DMF, 1.0 mmol, 20 eq) for terminal chloroacetylation. For selective deprotection of methoxytrityl group of Cys residue, the resins were treated with 2 mL of a solution of a solution of 2% trifluoroacetic acid (TFA), 5% triisopropylsilane (TIS) in DCM and shaken for 2 minutes followed by removal of the solution. This cycle was repeated 10 times for thorough deprotection of methoxytrityl group. After washed, the beads were treated with 10% DIPEA in DMF for neutralization (RT, 10 minutes). The linear peptoid loaded resins were then treated with 2M DIPEA in DMF overnight at RT for macrocyclization. Crude cyclic peptoids were recovered from the resin by incubation with a cleavage cocktail containing 95% TFA, 2.5% TIS and 2.5% water for 2 h at RT. All peptoids were then purified with HPLC using Zorbax C₁₈ (3 μm, 4.6 x 150 mm) column as the stationary phase. For the mobile phase, buffer A (water with 0.1% v/v TFA) and buffer B (acetonitrile with 0.1% v/v TFA) were used as a gradient.

1.2 Synthesis of TAMRA-labeled peptoids

TAMRA-labeled peptoids were synthesized with the same procedure with the synthesis of unlabeled cyclic peptoids. Instead of Fmoc-Cys(4-methoxytrityl)-OH, Fmoc-Lys(4-methoxytrityl)-OH (100 mg, 0.16 mmol) solution was added with PyBOP (92.1 mg, 0.18 mmol) and DIPEA (22.9 μL, 0.13 mmol) in 5 mL of DMF and irradiated for 5 min using microwave (ramping time for 2 min) at 5 W power.

Amine of this Lys will be conjugated with 5(6)-TAMRA (5-(and 6)-Carboxytetramethylrhodamine) at the end of the synthesis. After washing step, Fmoc protection group was removed by 5 mL of 20% piperidine in DMF by irradiating for 2min using microwave. After washing, the solution of Fmoc-NH-PEG-COOH (9 atoms) (60 mg, 0.16 mmol), PyBOP (92.1 mg, 0.18 mmol), DIPEA (22.9 μ L, 0.13 mmol) were added and irradiated for 5 min. After washing, Fmoc deprotection and another washing step, Fmoc-Cys(tert-butylthio)-OH (67.3 mg, 0.16 mmol), PyBOP (92.1 mg, 0.18 mmol), DIPEA (22.9 μ L, 0.13 mmol) were added to the resins and irradiated with microwave for 5 min. After Fmoc deprotection, coupling of peptoid monomers was performed using the same procedure used in the synthesis of unlabeled peptoids. After CAA coupling and washing step, tert-butylthio protection group of Cys was deprotected by modified Beekman protocol.⁴³ In brief, the resins were moved to 5 mL round bottom flask and tributylphosphine (32.5 μ L, 0.13 mmol) in NMP (N-methyl pyrrolidone) : water = 9:1 (1620 μ L: 180 μ L) was added and stirred for 1 h in N₂. After washing step, same procedure was repeated with 10 equivalents (65 μ L, 0.26 mmol) of tributylphosphine instead of 5 equivalents. Cyclization and Mmt deprotection were performed with the same procedure used in the synthesis of unlabeled peptoids. The solution of 5, (6)-TAMRA (44.8 mg, 0.1 mmol), N-Hydroxybenzotriazole (HOBt, 14.1 mg, 0.1 mmol), 2-(6-Chloro-1H-benzotriazole-1-yl)-1,1,3,3-tetramethylammonium hexafluorophosphate (HCTU, 43 mg, 0.1 mmol), DIPEA (30.5 μ L, 0.17 mmol) was added to the resins for the TAMRA coupling (2 h, RT). All TAMRA-labeled peptoids were then purified with the same HPLC methods used in the purification of unlabeled peptoids.

1.3 Synthesis of Cy5.5-labeled peptoid

Synthesis of Cy5.5-labeled peptoid I11 was performed following the same procedure with the synthesis of TAMRA-labeled peptoids. At the final step, instead of 5, (6)-TAMRA and other reagents, the solution of Cyanine 5.5 NHS ester (11.7 mg, 0.015 mmol), DIPEA (3.1 μ L, 0.02 mmol) in 1 mL of DMF was added to the *ca.* 20 mg resins (O/N, RT).

2. Anti-inflammatory activity

Jurkat cells were maintained in RPMI medium supplemented with 10% fetal bovine serum, penicillin, streptomycin at 37 °C in a 5% CO₂ incubator. To monitor the expressed mRNA levels of the proinflammatory cytokine interleukin 2 (IL-2), Jurkat cells (4×10^5 cells) were treated with 10 ng/mL of Phorbol 12-myristate 13-acetate (PMA) and 1 μ g/mL of ionomycin in the presence of 40 μ M of cyclic peptoids for 6 h at 37 °C in a 5% CO₂ incubator. As a positive control, 10 nM of CsA was used. The cells were then centrifuged at 14,000 rpm for 2 min at 4 °C and the supernatants were removed. The total RNA was isolated using TRIzolTM Reagent (InvitrogenTM) following the manufacturer's instruction. The isolated RNA was quantified with multimode microplate reader (Spark; TECAN) and 1 μ g of each was used to prepare the cDNA using TOPscriptTM RT DryMix (Enzynomics). Treated with RNase H, the cDNA was incubation for 20 min at 37 °C. The expressed IL-2

level of each sample was examined using TOPreal™ qPCR 2× PreMIX (Enzynomics, #RT500M) following a modified manufacturer's instruction. The housekeeping gene GAPDH was used as a reference for qPCR. The qPCR was performed with real-time PCR cycler (Rotor-Gene Q, QIAGEN).

3. Binding affinity measurement

1.1 Surface Plasmon Resonance (SPR)

The binding experiment were performed at BIACORE 3000 (GE Healthcare). Phosphate buffered saline (PBS) was used as a running buffer for the entire SPR assay. Carboxylic acids on the surface of CM5 sensor chip were activated by a mixture of equivalent volume of EDC (0.4 M) / NHS (0.1 M). A solution of streptavidin (1 mg/mL) was 1,000-fold diluted in sodium acetate (pH 5.5) and immobilized on both analyzing channel and the reference channel by the amine coupling method. Streptavidin (*c.a.* 5,000 RU) was immobilized at each flow channel. For further immobilization of biotinylated CypA and biotin on each channel, CypA and biotin were diluted in PBS before injection. CypA were immobilized at 3200 RU and 2600 RU for two independent experiments. Then, 10 mM of each cyclic peptoid in DMSO was diluted to 20 μM in PBS and analyzed for SPR screening. As a negative control, 0.2% DMSO in PBS was used.

1.2 Fluorescence Anisotropy

The binding constant of the peptoid to Cyps was determined by fluorescence anisotropy titration as previously described. To monitor fluorescence anisotropy change of 5-TAMRA-labeled peptoids upon addition of CypA (Sino Biological, #10436-H08E) or CypD (LifeSpan Biosciences, LS-G3522), 20 or 40 nM 5-TAMRA-peptoids in 35 mM HEPES buffer (10 mM NaCl, pH = 7.8) were used as the fluorescence probes. The probe solution was excited at 550 nm and monitored at 580 nm (each band path 10 nm) at 25 °C in a final volume of 500 μ L using a LS55 fluorescence spectrometer (Perkin Elmer) equipped with a thermo-controlled water circulator. The integration time was 10 s. A solution of CypA (or CypD) was added and the anisotropy was monitored at each concentration of CypA (or CypD). The average results of 5 measurement were used and binding affinities were calculated using Prism 8 (GraphPad Software Inc.) by an equation below.

$$A = A_0 + \Delta A \left\{ \frac{([Cyp] + [Peptoid]_0 + K_D) - \left(([Cyp] + [Peptoid]_0 + K_D)^2 - 4[Cyp][Peptoid]_0 \right)^{1/2}}{2[Peptoid]_0} \right\}$$

Where A and A₀ are the fluorescence anisotropy of labeled peptoids in the presence and absence of Cyps, respectively. ΔA is the fluorescence anisotropy in the presence of Cyp minus in the absence of Cyp. [Cyp] and [Peptoid]₀ are the concentrations of Cyp and initial peptoid respectively.

4. Blood-brain barrier (BBB) permeability measurement

The BBB permeability of the peptoids and CsA were analyzed using parallel artificial membrane permeability assay (Corning, cat. 353015). The experiment was triplicated. Five μL of 2% (w/v) brain polar lipid extract (Avanti, cat. 141101P) in dodecane was loaded on the porous PVDF membrane carefully before use. Two hundred μL of 100 μM peptoids and CsA in 5% DMSO in PBS were loaded on each donor well. On each acceptor well, 300 μL of PBS with 5% DMSO was loaded. After 16 h at room temperature, the concentrations of each well were determined using a HPLC (Agilent 1100 series). The concentrations of peptoids and CsA were determined from the calibration curves obtained from serial diluted solutions of each compound. A reverse phase C_{18} (3 μm , 4.6 x 150 mm) column was used as the stationary phase. For the mobile phase, buffer A (water with 0.1% v/v TFA) and buffer B (acetonitrile with 0.1% v/v TFA) were used as a gradient. The gradient conditions are as follows: linear gradient 40-60% B over 10 min. In case of CsA, linear gradient of buffer C (Water:ACN:MeOH=64:34:3) was used at 65 $^{\circ}\text{C}$.

5. Mitochondrial membrane potential recovery (JC-1)

5.1 Microplate reader

A JC-1 kit (Sigma CS0390A) was used to measure the difference of mitochondrial membrane potential ($\Delta\psi_m$) in SH-SY5Y cells according to the manufacturer's protocol. Briefly, a solution of JC-1 dye in Staining Solution

(Sigma CS0390) 3 mL was added to a suspension of SH-SY5Y cells (3×10^6 cells in 3 mL in DMEM complete media) and incubated with final 2 μ M of JC-1 dye (Sigma T4069) for 20 min at 37 °C. Mitochondrial membrane potential, represented as JC-1 ratio, was determined by measuring fluorescence intensity at excitation 485 nm, emission 590 nm for red fluorescence (J-aggregate) and at excitation 485 nm and emission 526 nm for green fluorescence (JC-1 monomer) using a microplate reader (Tecan Spark®) at 37 °C. Ratio red/green fluorescence 15 min after adding antimycin A, CsA or I11 was calculated for each condition. A total of three independent experiments were performed and each experiment was duplicated.

5.2 Confocal Laser Scanning Microscopy (CLSM)

SH-SY5Y cells (5×10^4 cells/well) were seeded on a 35 mm x 10 mm confocal dish (SPL, 200350) and incubated 24 h. Cells were stained with JC-1 (2 μ M) at 37 °C for 15 minutes and washed with complete DMEM media. Antimycin A (20 μ M), CsA (1 μ M) and I11 (1 μ M) were treated to each sample for 15 minutes. After PBS washout, cells were observed using confocal laser scanning microscope (Zeiss, LSM 880) with 40x lens. For the measurement of JC-1 monomer intensity, 488 nm laser was used with the filter range of 493 nm - 544 nm. For the J-aggregate, 561 nm laser was used with the filter range of 577 nm - 631 nm.

6. Cell viability assay

SH-SY5Y cells (1.0×10^4 cells/well) were seeded on a 96-well plate and incubated 24 h. Cells were incubated with final 10 μ M of each peptoid in 5% DMSO in DMEM

media. After incubation at 37 °C for 24 h, cell viability was analyzed using WST-1 assay (DoGen, cat. EZ-3000). Absorbance of each well was measured at 450 nm using a multimode microplate reader (TECAN, Spark). The viability was calculated by the ratio of the absorbance of chemical treated cells to that of not treated cells.

7. Biodistribution

Four hundred μM of Cy5.5-I11 was prepared in a vehicle solution (saline:Tween-20:DMSO=83.3:10:6.7). One hundred twenty five μL (0.05 μmol , 86.9 μg) was injected intravenously to 6 week old BALB/c nude mice via tail (n=3). While the mice being anesthetized with isoflurane in oxygen gas, in vivo imaging was performed with IVIS Spectrum CT (Perkin Elmer) using instrumental settings for Cy5.5 dye. Mice were sacrificed 230 min post-injection, and then brain, kidney, heart, spleen, lung and liver were collected from each mouse without delay. Fluorescence intensity of Cy5.5-I11 in each organ was measured and its biodistribution (%) was calculated by the ratio of total radient efficiency $[(\text{p}/\text{sec}/\text{cm}^2/\text{sr})/(\mu\text{W}/\text{cm}^2)]$ for each organ to the total radient efficiency sum of analyzed six organs.

Results and Discussion

Design and Synthesis of macrocyclic peptoid library.

Macrocyclic peptoid library, chosen to screen to target protein CypA, was constructed using ten different amines which substitute bromide of bromoacetic amide to form *N*-substituted glycines. Amines were incorporated to the OBOC library five times by split-and-pool method, thus composed of cyclic 5 peptoid monomers with theoretical diversity of 10^5 . Three groups of monomeric amines were chosen, composed of two linear aliphatic amines (X group), two cyclic amphiphatic amines (Y group), and six aromatic amines (Z group) (Fig. 2) among commonly used amine residues for peptoid library.⁴⁴ Thereby, the cyclic penta-peptoids achieve the hydrophobicity to bind to the binding pocket. The structural diversity made in the peptoid library also allowed for the determination of binding affinity variation against target protein within each respective sequence.

TentaGel® B Boc/NH₂ (Rapp Polymere, #B30902.12) bi-functional resin was used for screening and identification of selected peptoids at the same time. Linear peptoids and cyclic peptoids were loaded respectively on free amine residues inside and BOC protected residues outside, as shown in Fig. 3 (details in Fig. 4). Thereby, the cyclic peptoids were readily exposed to bind to the target protein, and the linear peptoids inside the resin corresponding to the sequences of the cyclic peptoids were designated to be sequenced by CNBr cleavage.

Library screening and selection of cyclic peptoids binding to CypA.

CypA was chosen as a target protein for peptoid library screening, since CypA is a major target of CsA and easily expressed stable protein among Cyp isoforms. It was hypothesized that the similarity of CypA and CypD would allow CypA binding peptoids to bind both isoforms and have mitochondrial membrane potential recovery potency as well as anti-inflammatory properties. Streptavidin-conjugated magnetic bead (Dynabeads™ M-270 Streptavidin, Thermo Fisher Scientific) was used to screen the peptoids binding to biotinylated CypA. Biotinylation was performed using activated biotinylation reagent, EZ-Link™ Sulfo-NHS-LC-LC biotin (Thermo Scientific). Before selection, magnetic beads were incubated with StartingBlock™ (Thermo Scientific) to remove nonspecific binders. The tight binding peptoids to CypA were pulled out using a magnet by eliminating the unbound and weak binding peptoids through thorough washing step (Fig. 1). Among 10⁵ OBOC library, 100 beads were selected out by affinity with streptavidin-coated magnetic beads.⁴⁵ Each peptoid was sequence analyzed using MS/MS sequencing method (Table 1). To obtain sufficient lipophilicity and hydrophobicity, peptoids including at least two aromatic peptoid monomer (*Z* group) amines were preferred. Thereby, each cyclic peptoid was selected in the following criteria. First, it included at least two aromatic peptoid monomers in *Z* group (88 peptoids out of 100 selected peptoids), but rejected consecutive *Z* to avoid crowdedness (28 peptoids). Second, at least two aliphatic peptoid monomers in *X* group and one Nleu were included (10 peptoids) to mimic CsA binding since two N-methyl-leucines of CsA are involved in binding to CypA.⁴⁶

Finally, highly graded 10 cyclic peptoids were individually synthesized and used for further studies (Table 2, Fig. 5-8).

Figure 1. OBOC cyclic peptide library construction and screening of CypA inhibitors.

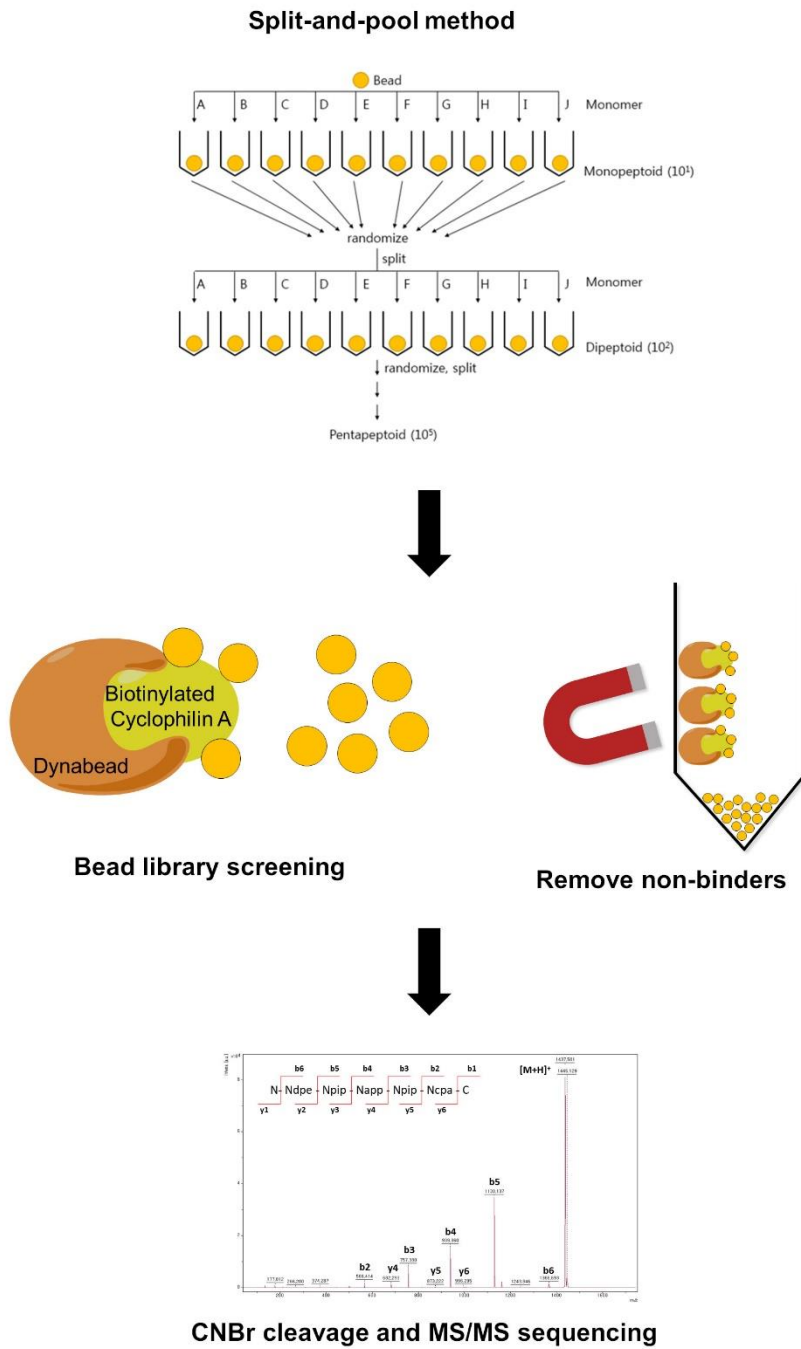


Figure 2. Amine monomers for peptoid library construction.

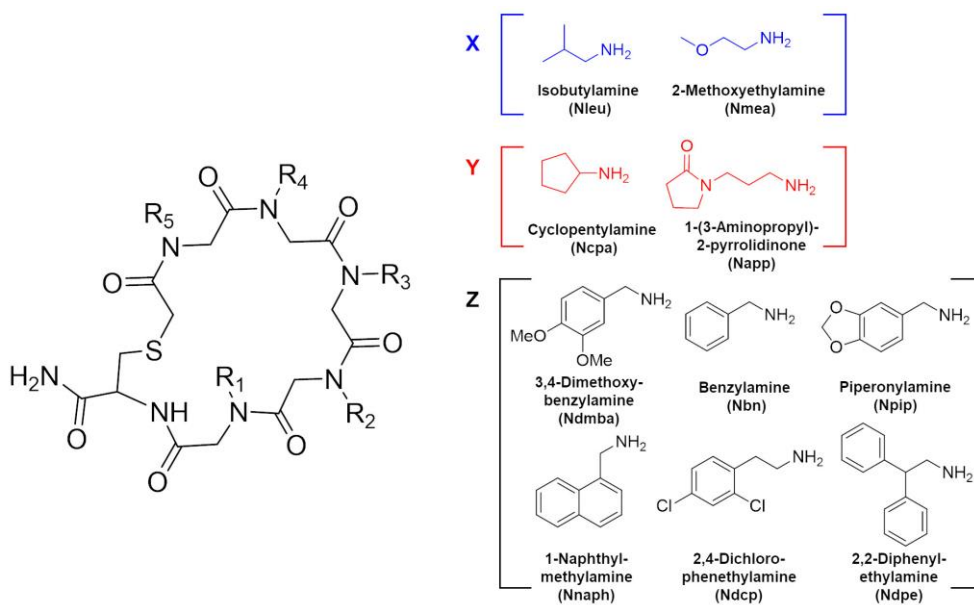


Figure 3. General scheme for the construction of sequenceable OBOC cyclic peptoid library using bi-functional resin.

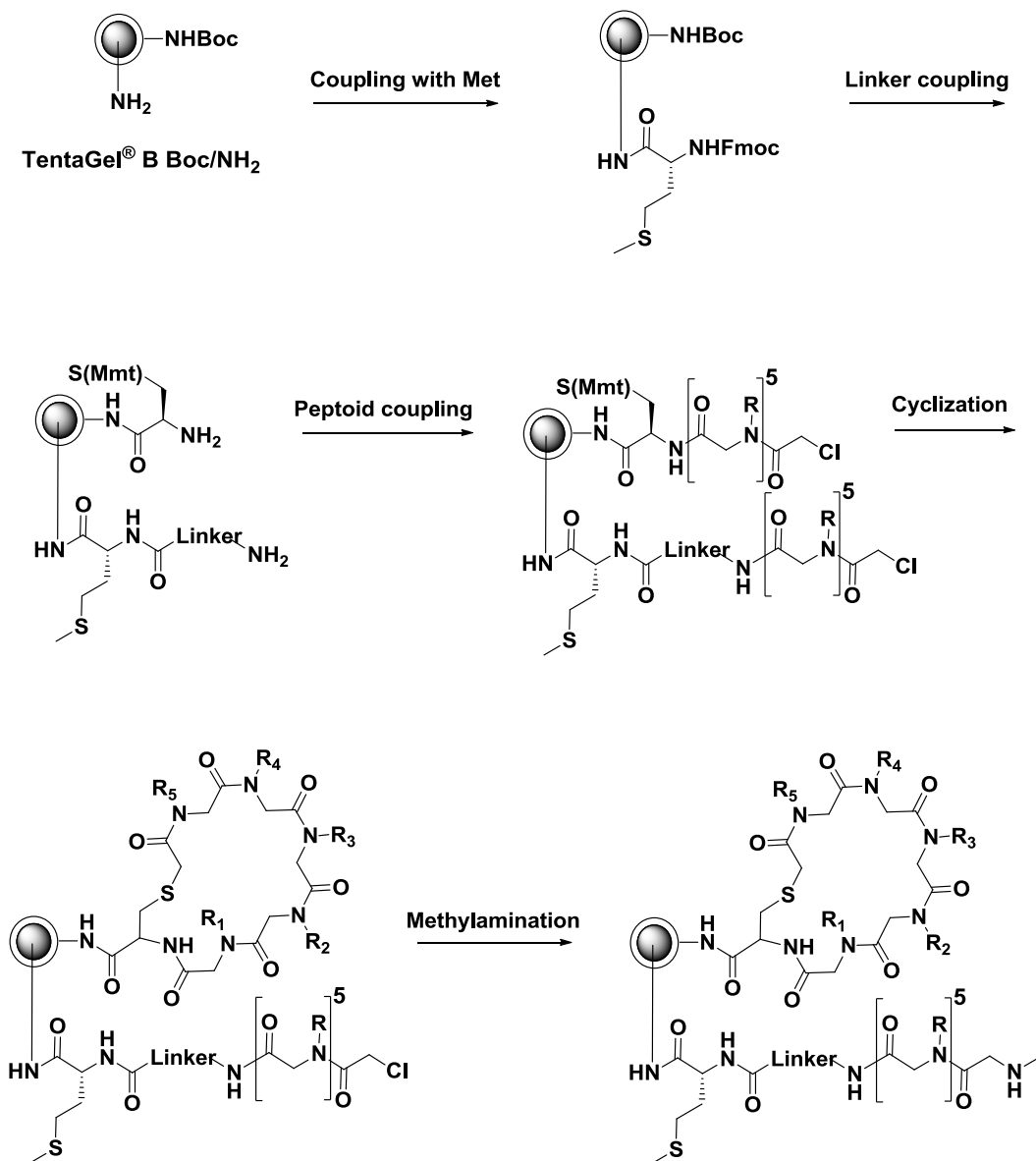


Figure 4. Synthetic details for the construction of sequenceable OBOC cyclic peptoid library using bi-functional resin.

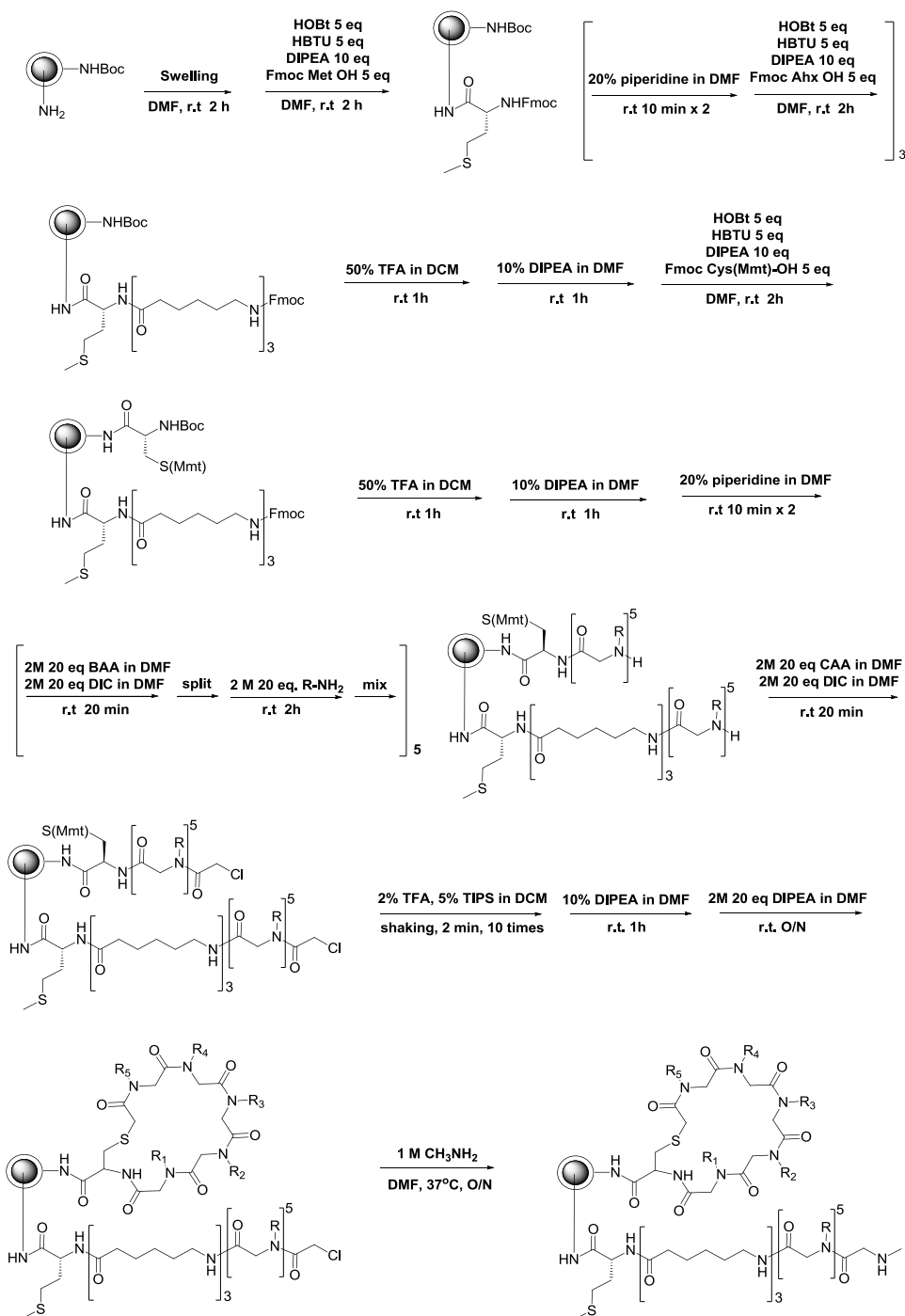


Table 1. Names and sequences of 100 peptoids.

Sequence #	Name of sequence	Position of monomer					Sequence #	Name of sequence	Position of monomer				
		1	2	3	4	5			1	2	3	4	5
1	F1	Nbn	Ndmba	Ndmba	Ncpa	Ncpa	51	H3	Npip	Nmea	Nleu	Napp	Ndmba
2	F2	Ndpe	Npip	Napp	Npip	Ncpa	52	H4	Nnaph	Nmea	Ncpa	Ndmba	Ncpa
3	F3	Ndmba	Nbn	Nmea	Nbn	Nnaph	53	H5	Ndpe	Ncpa	Ndmba	Npip	Ndmba
4	F4	Nmea	Nbn	Napp	Ndcp	Ncpa	54	H6	Ndmba	Nmea	Ndmba	Npip	Nbn
5	F5	Nmea	Nbn	Ncpa	Ncpa	Napp	55	H7	Nmea	Nleu	Nbn	Nnaph	Nmea
6	F6	Nnaph	Npip	Napp	Nmea	Nbn	56	H8	Nbn	Nleu	Napp	Nbn	Ndmba
7	F7	Napp	Ndmba	Nnaph	Npip	Npip	57	H9	Npip	Nleu	Nnaph	Nmea	Npip
8	F8	Ndcp	Npip	Nmea	Ncpa	Nmea	58	H10	Nbn	Ndmba	Nbn	Nbn	Nmea
9	F9	Napp	Nbn	Ncpa	Ndmba	Npip	59	H11	Ndcp	Nleu	Nmea	Ncpa	Ndpe
10	F10	Npip	Nmea	Napp	Ndpe	Npip	60	H12	Nnaph	Napp	Npip	Ncpa	Ndmba
11	F11	Nmea	Ndpe	Napp	Ncpa	Nnaph	61	H13	Ndcp	Nleu	Ndmba	Nbn	Nmea
12	F12	Ndpe	Ndcp	Napp	Nleu	Nmea	62	H14	Nleu	Nmea	Napp	Ndmba	Ncpa
13	F13	Ndmba	Ndmba	Nnaph	Napp	Nbn	63	H15	Nnaph	Ndpe	Nbn	Ncpa	Nmea
14	F14	Nnaph	Napp	Nnaph	Nmea	Ndmba	64	H16	Ncpa	Napp	Ncpa	Ndcp	Nbn
15	F15	Nleu	Nleu	Nleu	Nmea	Ndpe	65	H17	Ndcp	Nmea	Nleu	Nmea	Ndcp
16	F16	Nbn	Nmea	Nleu	Nnaph	Ndpe	66	H18	Nmea	Ncpa	Nnaph	Nbn	Ncpa
17	F17	Ndmba	Nbn	Nnaph	Nbn	Nleu	67	H19	Nnaph	Nleu	Napp	Ndcp	Napp
18	F18	Ncpa	Nmea	Ndpe	Ncpa	Nbn	68	H20	Napp	Ndmba	Ndmba	Nmea	Ndpe
19	F19	Nbn	Nnaph	Ncpa	Ncpa	Ndmba	69	H21	Nnaph	Napp	Nmea	Ndmba	Npip
20	F20	Ndmba	Npip	Npip	Ncpa	Ndpe	70	H22	Nnaph	Nnaph	Nnaph	Nleu	Nmea
21	F21	Ndmba	Nleu	Ncpa	Nbn	Ndmba	71	H23	Ndcp	Nleu	Ncpa	Nmea	Ndmba
22	F22	Ncpa	Npip	Nmea	Ncpa	Nmea	72	H24	Nnaph	Napp	Nleu	Napp	Ncpa
23	F23	Napp	Ndcp	Nmea	Ndmba	Ndpe	73	I1	Ndpe	Nnaph	Ncpa	Ncpa	Nbn
24	F24	Ndmba	Nleu	Ncpa	Nbn	Ndmba	74	I2	Ncpa	Ndcp	Nmea	Ndmba	Napp
25	G1	Nnaph	Ndmba	Nleu	Ncpa	Napp	75	I3	Ncpa	Napp	Nmea	Nnaph	Ndpe
26	G2	Ncpa	Nleu	Nbn	Nnaph	Napp	76	I4	Npip	Nmea	Nleu	Napp	Ndmba
27	G3	Ndmba	Ndpe	Ncpa	Ndmba	Napp	77	I5	Npip	Npip	Nleu	Ndpe	Ncpa
28	G4	Ndpe	Nmea	Ncpa	Nnaph	Napp	78	I6	Nnaph	Napp	Nnaph	Nleu	Napp
29	G5	Npip	Ndmba	Ndpe	Nmea	Nnaph	79	I7	Nmea	Nbn	Nbn	Nleu	Nnaph
30	G6	Nleu	Nnaph	Ndcp	Nnaph	Napp	80	I8	Ncpa	Nleu	Ndmba	Nnaph	Ndmba
31	G7	Ncpa	Nbn	Ncpa	Nleu	Npip	81	I9	Ndmba	Ndmba	Ncpa	Nnaph	Napp
32	G8	Npip	Nmea	Ndpe	Nnaph	Napp	82	I10	Ndcp	Napp	Ncpa	Ndmba	Nbn
33	G9	Ndmba	Ndpe	Nbn	Napp	Napp	83	I11	Nleu	Nnaph	Nleu	Ncpa	Npip
34	G10	Npip	Nbn	Nbn	Npip	Npip	84	I12	Nbn	Nmea	Nbn	Nbn	Nmea
35	G11						85	I13	Nnaph	Ndpe	Ndpe	Ndmba	Ndpe
36	G12	Nnaph	Ndmba	Nmea	Ndcp	Ncpa	86	I14	Ndcp	Ncpa	Nbn	Nleu	Nmea
37	G13	Ndmba	Ndmba	Nnaph	Ncpa	Ndmba	87	I15	Ncpa	Nleu	Ndcp	Nleu	Ndmba
38	G14	Napp	Nleu	Napp	Ndcp	Nmea	88	I16	Ncpa	Ndmba	Ndcp	Napp	Nbn
39	G15	Napp	Ndmba	Ndcp	Nbn	Nmea	89	I17	Nmea	Nmea	Nbn	Nnaph	Ndmba
40	G16	Napp	Ndmba	Ncpa	Ncpa	Ndmba	90	I18	Npip	Ndmba	Nbn	Ndmba	Napp
41	G17	Napp	Ndcp	Ndcp	Napp	Ndmba	91	I19	Napp	Ncpa	Npip	Npip	Ndmba
42	G18	Napp	Nmea	Ndpe	Npip	Ndmba	92	I20	Napp	Nmea	Nbn	Ncpa	Ndmba
43	G19	Nnaph	Ncpa	Npip	Npip	Ndmba	93	I21	Napp	Npip	Ndpe	Npip	Nmea
44	G20	Napp	Nnaph	Nbn	Nbn	Napp	94	I22					
45	G21	Nbn	Nnaph	Napp	Nbn	Napp	95	I23	Ndmba	Napp	Npip	Ncpa	Nmea
46	G22						96	I24	Npip	Nmea	Nmea	Npip	Nmea
47	G23	Napp	Nleu	Nbn	Napp	Nnaph	97	J1	Npip	Nleu	Napp	Nmea	Ndpe
48	G24	Nleu	Npip	Nmea	Nbn	Ndmba	98	J2	Napp	Ncpa	Nmea	Napp	Ndcp
49	H1	Nmea	Napp	Napp	Ndcp	Napp	99	J3	Ndpe	Ndcp	Napp	Ncpa	Nmea
50	H2	Nmea	Ndcp	Nnaph	Nnaph	Nmea	100	J4	Nnaph	Ncpa	Npip	Ncpa	Nnaph

Figure 5. Sequences and structures of 10 selected peptoids.

sequence #	Name of sequence	position of monomer				
		1	2	3	4	5
51	H3	Npip	Nmea	Nleu	Napp	Ndmba
57	H9	Npip	Nleu	Nnaph	Nmea	Npip
59	H11	Ndcp	Nleu	Nmea	Ncpa	Ndpe
65	H17	Ndcp	Nmea	Nleu	Nmea	Ndcp
71	H23	Ndcp	Nleu	Ncpa	Nmea	Ndmba
76	I4	Npip	Nmea	Nleu	Napp	Ndmba
83	I11	Nleu	Nnaph	Nleu	Ncpa	Npip
86	I14	Ndcp	Ncpa	Nbn	Nleu	Nmea
87	I15	Ncpa	Nleu	Ndcp	Nleu	Ndmba
97	J1	Npip	Nleu	Napp	Nmea	Ndpe

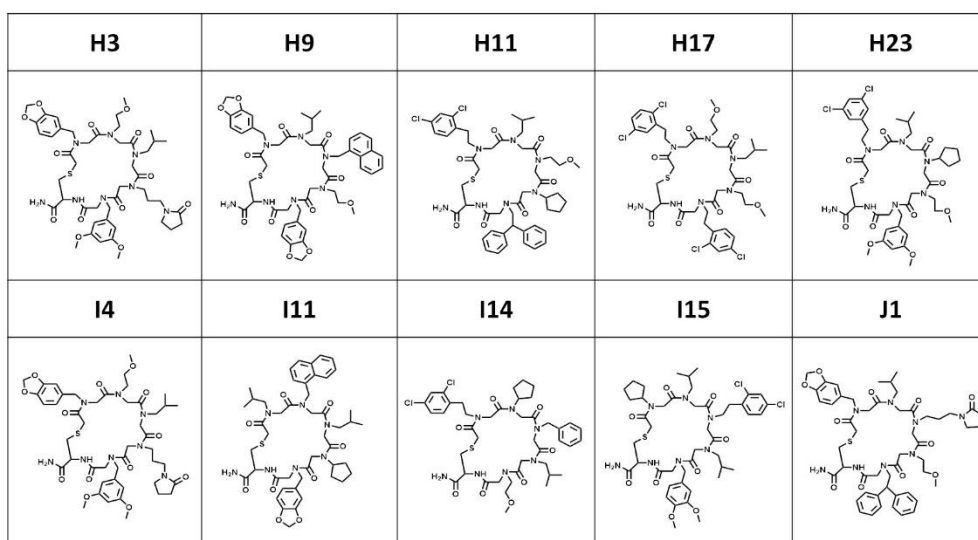


Figure 6. Synthetic scheme for cyclic peptoids.

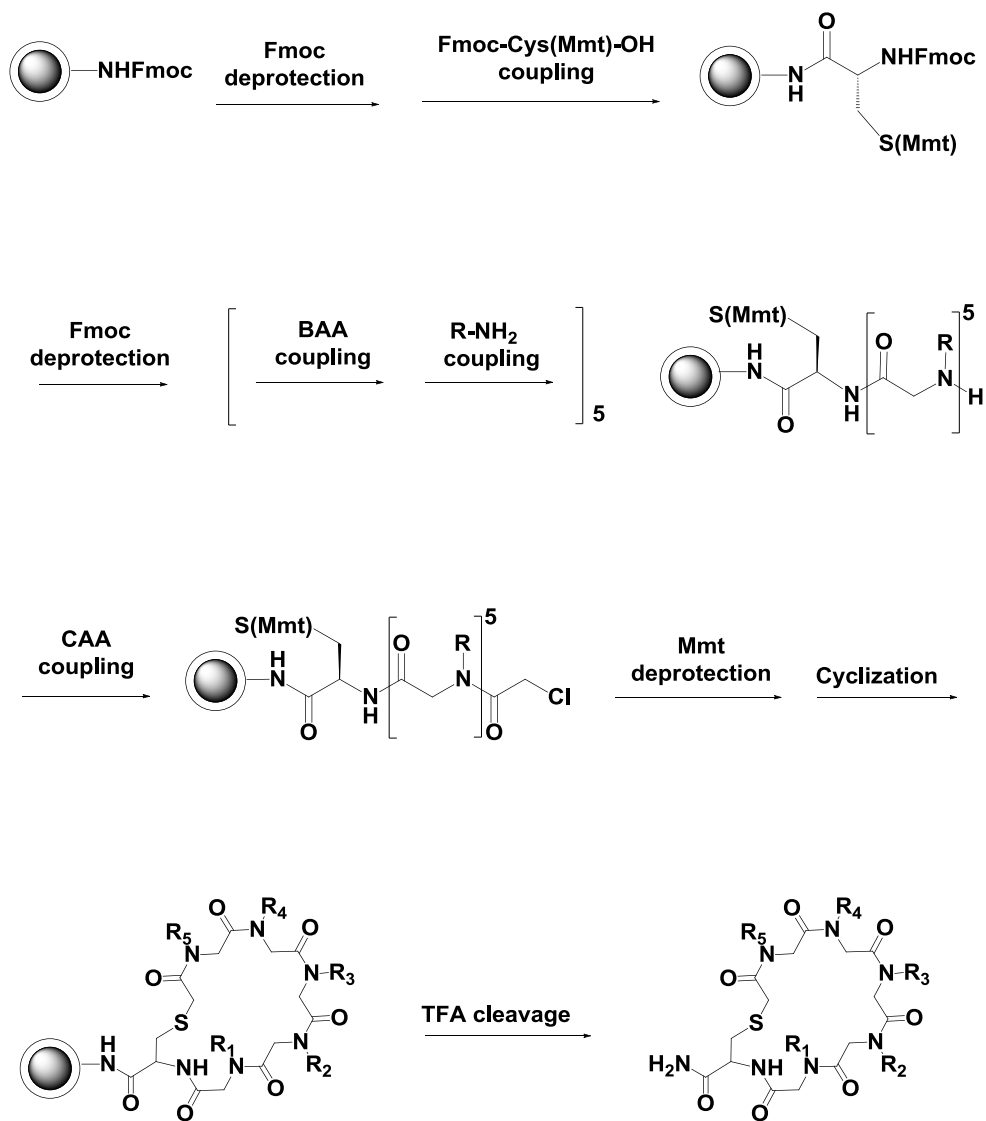


Figure 7. Synthetic details for cyclic peptoids.

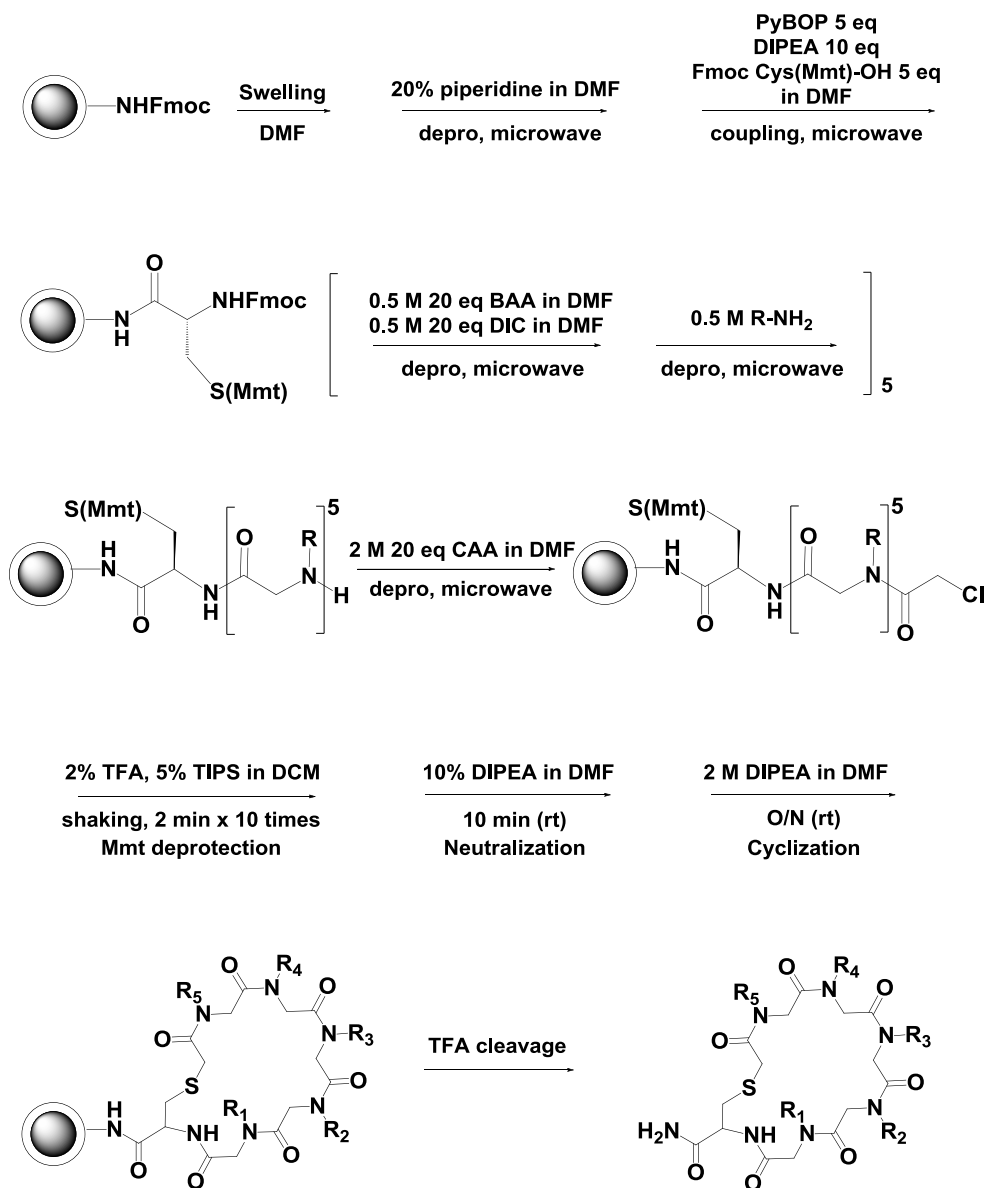
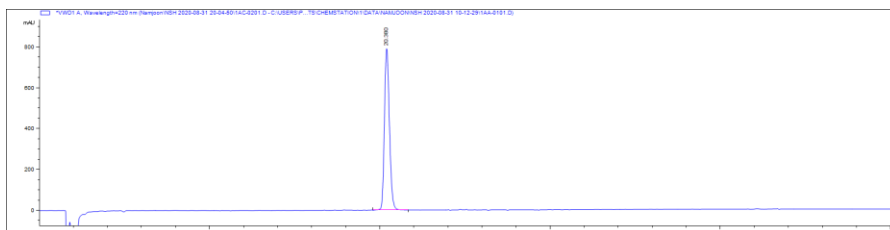
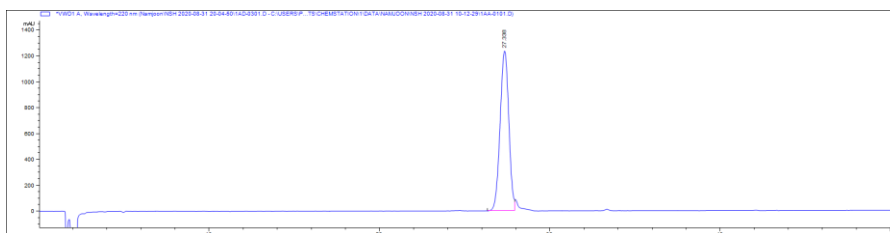


Figure 8. Chromatograms of cyclic peptoids

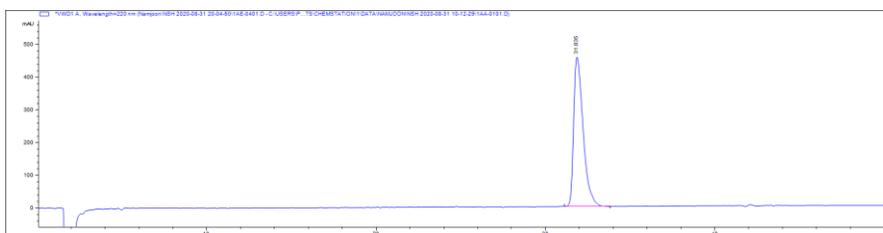
H3 was obtained as a white powder. The HPLC chromatogram of H3 is shown below (100% purity).



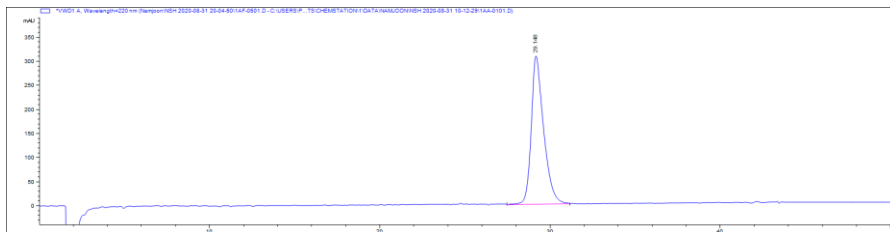
H9 was obtained as a white powder. The HPLC chromatogram of H9 is shown below (96% purity).



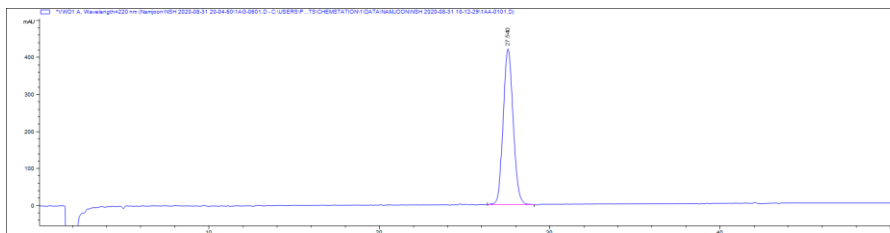
H11 was obtained as a white powder. The HPLC chromatogram of H11 is shown below (100% purity).



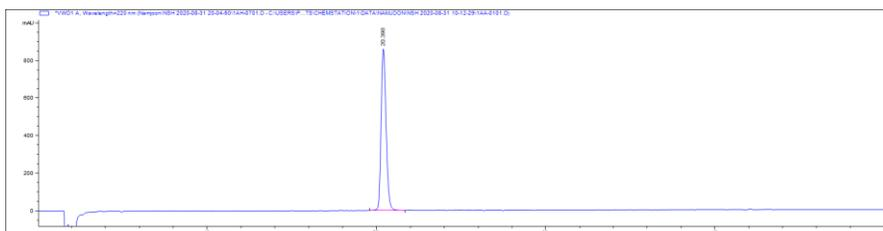
H17 was obtained as a white powder. The HPLC chromatogram of H17 is shown below (100% purity).



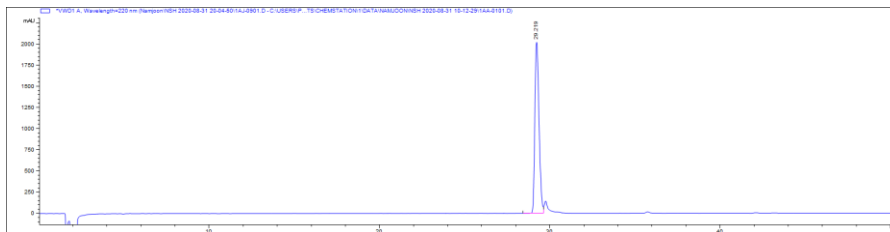
H23 was obtained as a white powder. The HPLC chromatogram of H23 is shown below (100% purity).



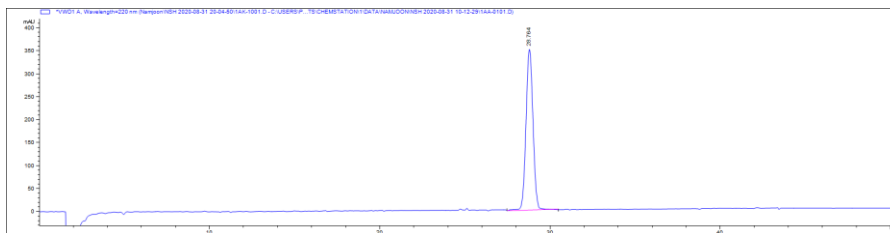
I4 was obtained as a white powder. The HPLC chromatogram of I4 is shown below (100% purity).



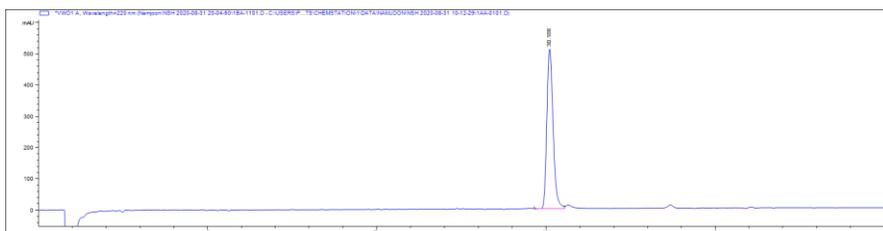
I11 was obtained as a white powder. The HPLC chromatogram of I11 is shown below (93% purity).



I14 was obtained as a white powder. The HPLC chromatogram of I14 is shown below (99% purity).



I15 was obtained as a white powder. The HPLC chromatogram of I15 is shown below (96% purity).



J1 was obtained as a white powder. The HPLC chromatogram of J1 is shown below (100% purity).

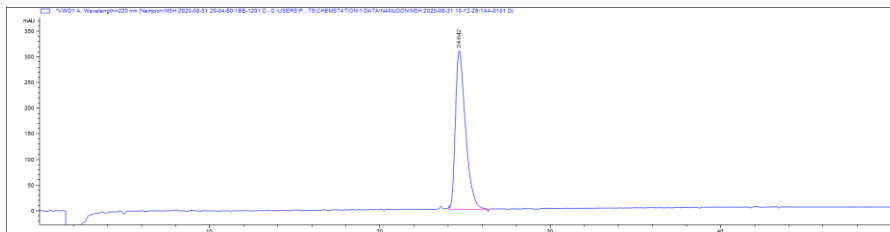


Table 2. Sequence and mass data of cyclic peptoids.

Peptoid	Sequence	MS [M+H] ⁺	
		Calcd.	Obsd.
H3	cyclo[Cys-N _{dmba} -N _{app} -N _{leu} -N _{mea} -N _{pip}]	969.43	969.63
H9	cyclo[Cys-N _{pip} -N _{mea} -N _{naph} -N _{leu} -N _{pip}]	968.38	968.60
H11	cyclo[Cys-N _{dpe} -N _{cpa} -N _{mea} -N _{leu} -N _{dcp}]	980.38	980.61
H17	cyclo[Cys-N _{dcp} -N _{mea} -N _{leu} -N _{mea} -N _{dcp}]	962.25	964.41
H23	cyclo[Cys-N _{dmba} -N _{mea} -N _{cpa} -N _{leu} -N _{dcp}]	950.36	950.49
I4	cyclo[Cys-N _{dmba} -N _{app} -N _{leu} -N _{mea} -N _{pip}]	969.43	969.60
I11	cyclo[Cys-N _{pip} -N _{cpa} -N _{leu} -N _{naph} -N _{leu}]	900.43	900.53
I14	cyclo[Cys-N _{mea} -N _{leu} -N _{bn} -N _{cpa} -N _{dcp}]	890.34	890.36
I15	cyclo[Cys-N _{dmba} -N _{leu} -N _{dcp} -N _{leu} -N _{cpa}]	948.38	948.51
J1	cyclo[Cys-N _{dpe} -N _{mea} -N _{app} -N _{leu} -N _{pip}]	999.46	999.52

Anti-inflammatory effects of selected peptoid

To evaluate the anti-inflammatory properties of cyclic peptoids interacting with the immunophilins, anti-inflammatory effects were screened against stimulated T cells. As it is known that the immunosuppressant drug, CsA, suppresses the expression of interleukin-2 (IL-2) as an index of T-cell immune response by the formation of CsA-CypA complex that inhibits calcineurin/nuclear factor of activated T cells (NFAT) signaling (Fig. 9). It was assumed that the cyclic peptoids might also show inhibition of IL-2 expression when bound to CypA. Anti-inflammatory effects were screened by determining the reduction of mRNA production of IL-2 stimulated with phorbol-12-myristate-13-acetate (PMA) and calcium ionophore in Jurkat cells. As previously reported, CsA at 10 nM strongly suppressed the mRNA expression of IL-2. In the presence of 40 μ M of cyclic peptoids, six out of ten cyclic peptoids showed over 50% inhibition effect (Fig. 10). As the most effective peptoid, I11 showed dose-dependent IL-2 inhibition as well (Fig. 11). The result showed that selected peptoids may form a complex with CypA, which consequently showed the repression of IL-2 expression. For further confirmation, binding affinities of these peptoids to CypA were monitored.

Figure 9. Schematic model for the inhibition of anti-inflammatory activity of CypA by CsA or cyclic peptides.

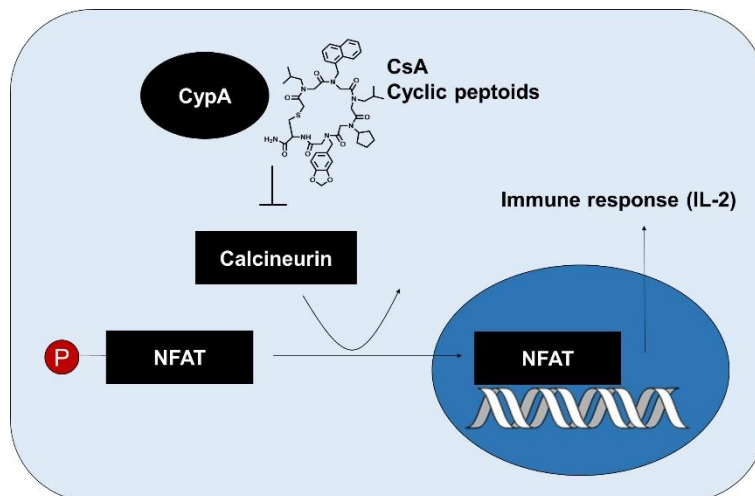
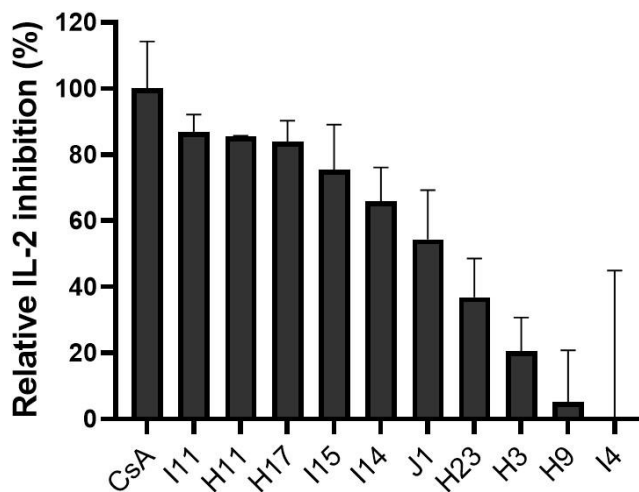
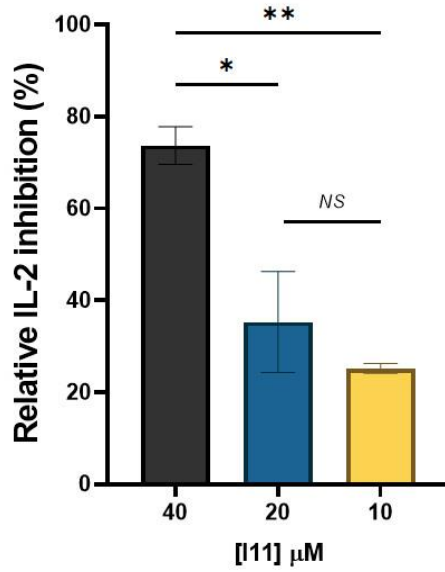


Figure 10. Relative IL-2 inhibition of selected cyclic peptides (40 μ M) presented as % of CsA (10 nM).



* All experimental data are shown as mean \pm SD (n=4).

Figure 11. Relative IL-2 inhibition of I11 as concentration-dependent manner.



* All data are shown as mean \pm SD (n=2); *P \leq 0.05; **P \leq 0.01; NS, not significant; Unpaired Student's t-test was performed using GraphPad Prism 8.

Binding affinity of peptoids to CypA

Next, I performed binding affinity measurements of cyclic peptoids to CypA by surface plasmon resonance (SPR) binding analysis (Fig. 12 - 14) and fluorescence anisotropy analysis (Table 4, Fig. 18). According to SPR results, relative binding efficiencies of the peptoids were positively correlated with the anti-inflammatory effects (Fig. 15, Spearman's $r = 0.782$, $P = 0.01$). Here, I confirmed the validity of initial experimental design to identify the inhibitors of CypA activity by screening CypA binders.

Four peptoids, effective in anti-inflammatory activities corresponding above 70% of inhibition efficiency, I11, H11, H17, and I15 were labeled with TAMRA fluorescent dye for the fluorescence anisotropy analysis (Table 3, Fig. 16 - 17). The results (Table 4, Fig. 18) confirmed that the most effective anti-inflammatory peptoid, I11, binds to CypA with $K_D = 150 \pm 30$ nM. Meanwhile, the binding affinity of CsA to CypA is shown as 81 ± 15 nM, which is similar with the previous report using intrinsic fluorescence intensity of Trp at the binding site.⁴⁷

Figure 12. Concept of SPR-based relative binding affinity screening.

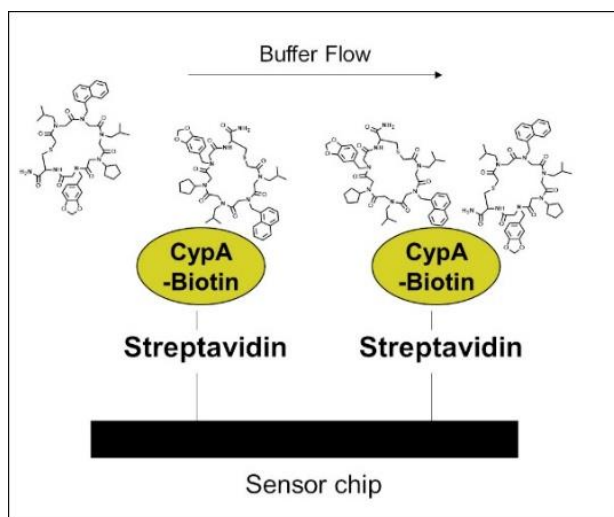


Figure 13. Representative SPR sensorgrams for the interaction of selected compounds with CypA.

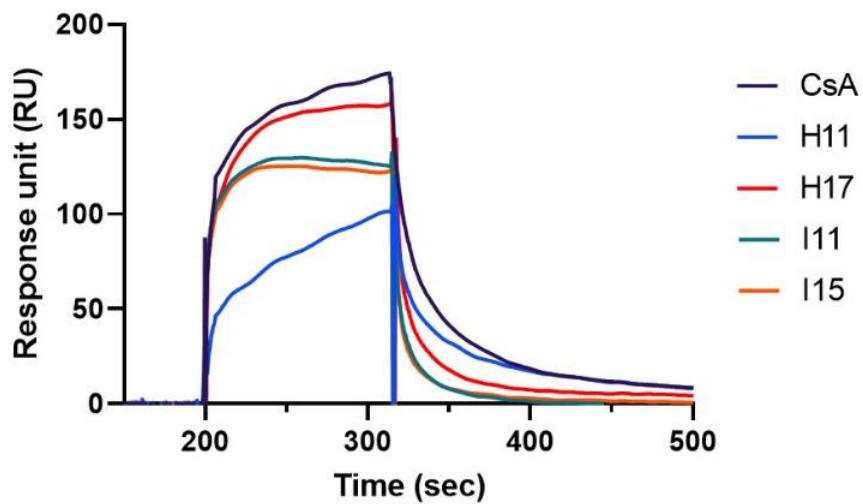
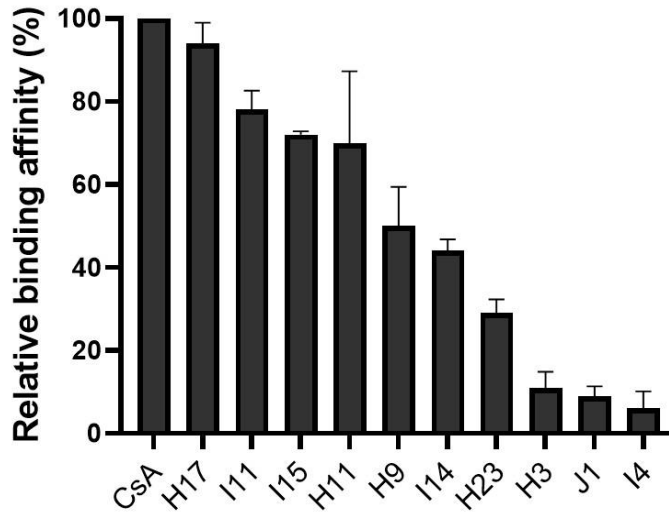


Figure 14. Relative binding affinity of cyclic peptoids presented as % of CsA.



* All experimental data are shown as mean \pm SD (n=2).

Figure 15. Correlation of binding affinity to CypA and IL-2 inhibition of cyclic peptoids.

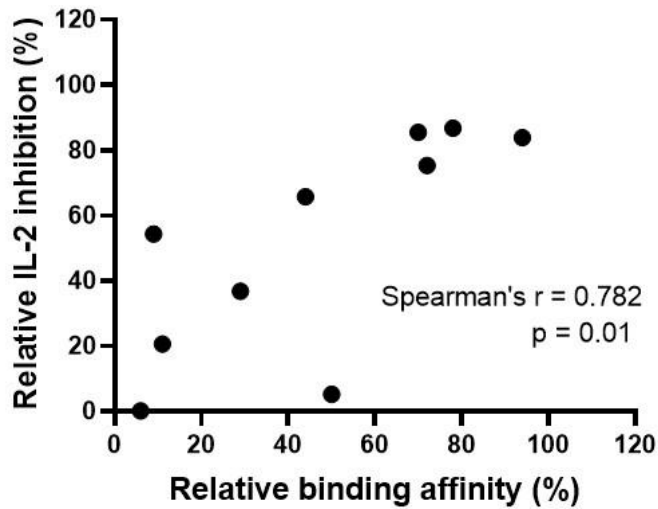
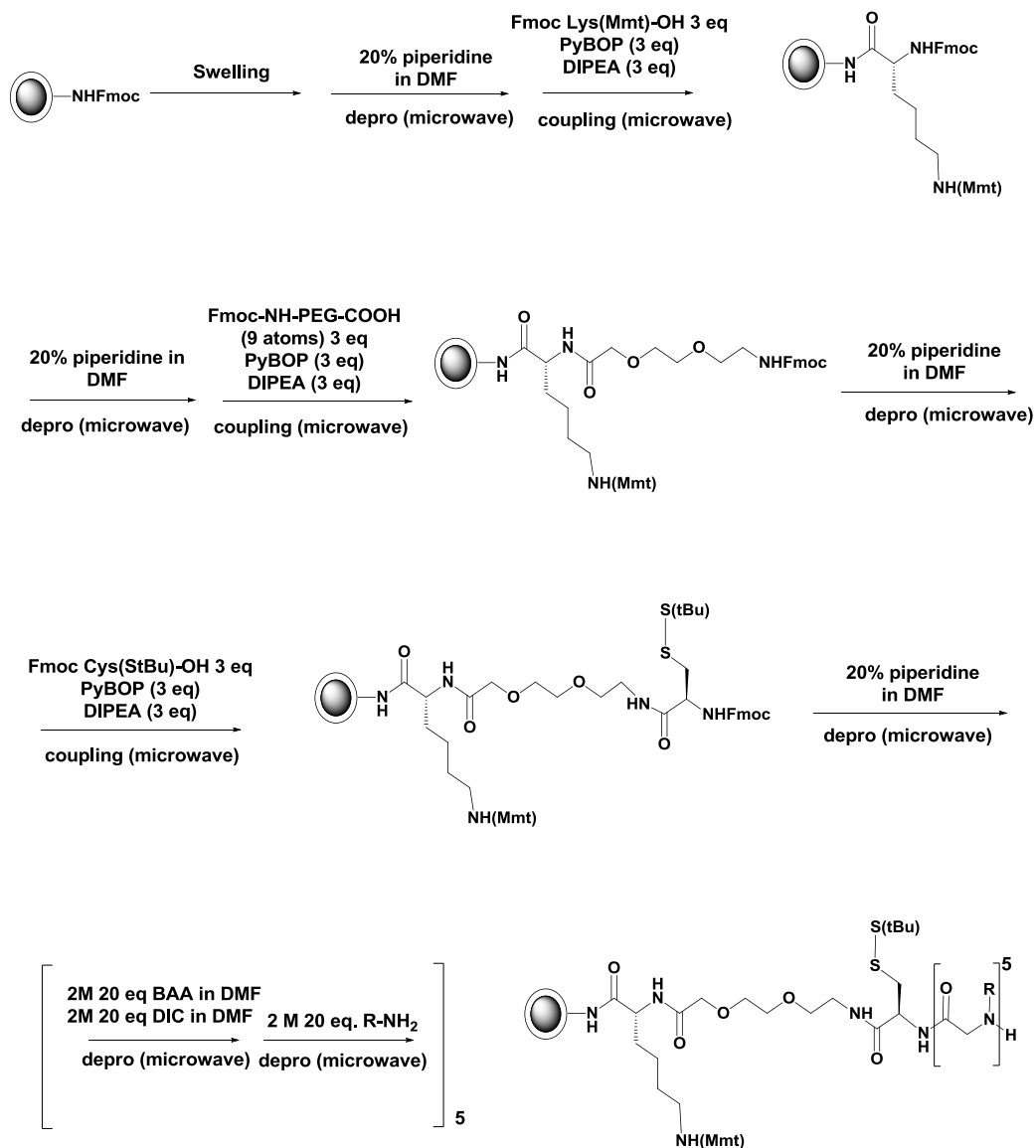


Figure 16. Synthetic details for TAMRA-labeled cyclic peptoids.



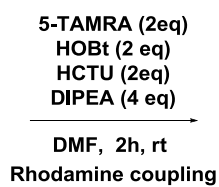
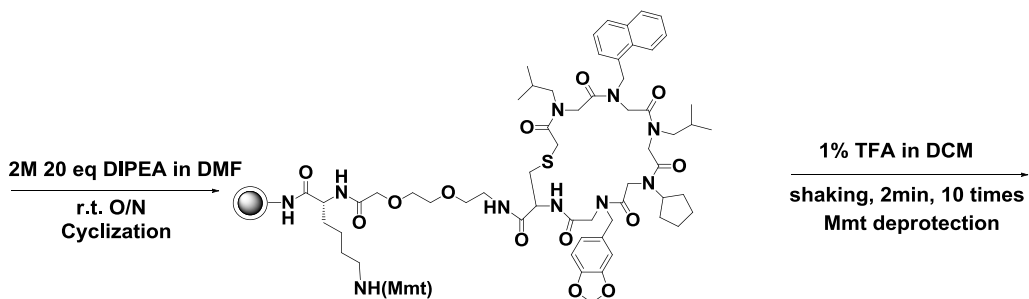
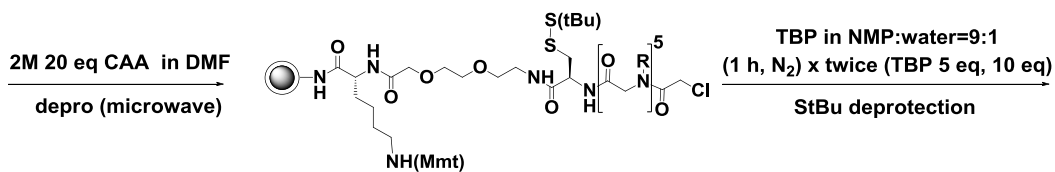
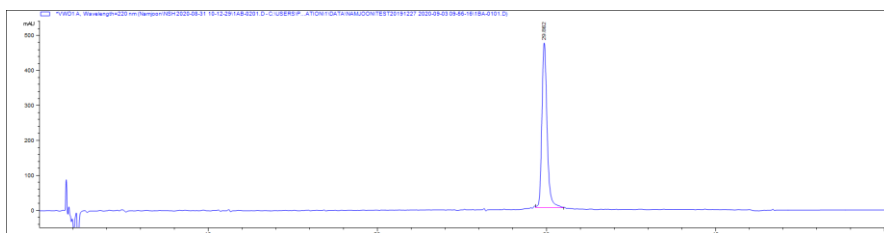
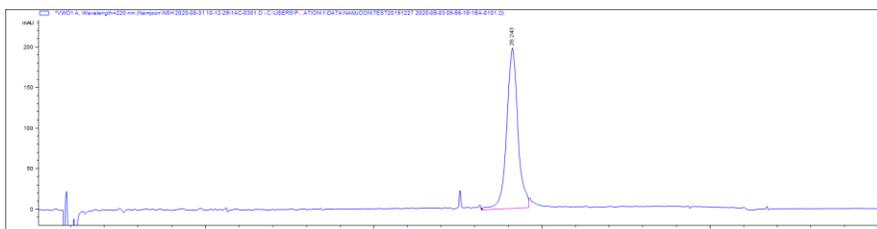


Figure 17. Chromatograms of TAMRA-labeled cyclic peptides.

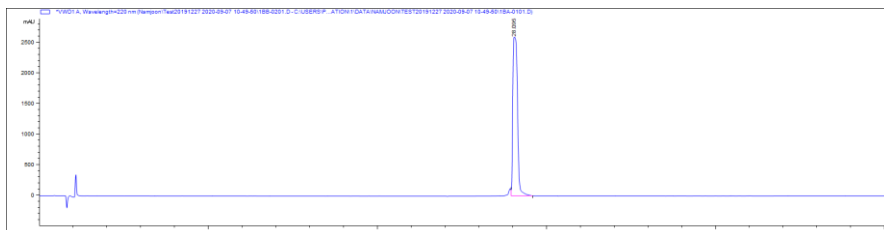
TAMRA-H11 was obtained as a red powder. The HPLC chromatogram of TAMRA-H11 is shown below (100% purity).



TAMRA-H17 was obtained as a red powder. The HPLC chromatogram of TAMRA-H17 is shown below (98% purity).



TAMRA-I11 was obtained as a red powder. The HPLC chromatogram of TAMRA-I11 is shown below (98% purity)



TAMRA-I15 was obtained as a red powder. The HPLC chromatogram of TAMRA-I15 is shown below (100% purity).

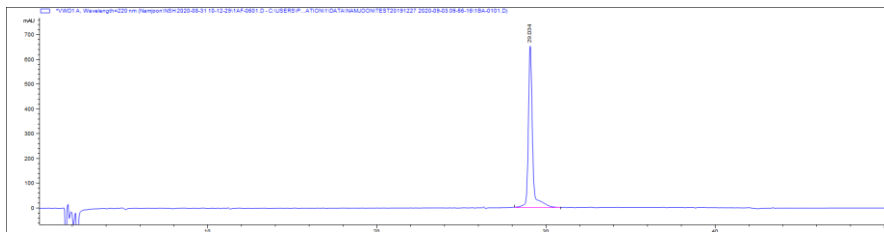


Table 3. Sequence and mass data of TAMRA-labeled peptoids.

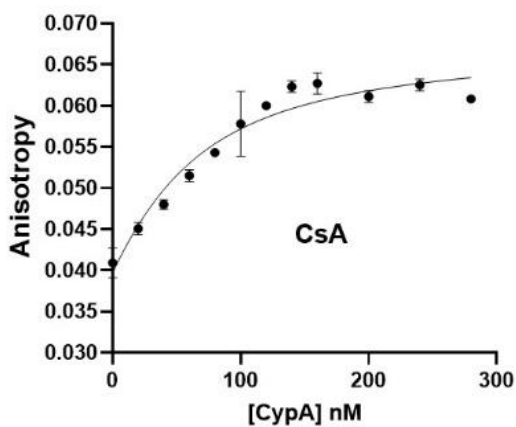
Peptoid	Sequence	MS [M+H] ⁺	
		Calcd.	Obsd.
TAMRA-H11	Rho-Lys-peg-cyclo[Cys-N _{dpe} -N _{cpa} -N _{mea} -N _{leu} -N _{dcp}]	1665.69	1665.16
TAMRA-H17	Rho-Lys-peg-cyclo[Cys-N _{dcp} -N _{mea} -N _{leu} -N _{mea} -N _{dcp}]	1647.56	1649.03
TAMRA-II1	Rho-Lys-peg-cyclo[Cys-N _{pip} -N _{cpa} -N _{leu} -N _{naph} -N _{leu}]	1585.74	1586.15
TAMRA-II5	Rho-Lys-peg-cyclo[Cys-N _{dmba} -N _{leu} -N _{dcp} -N _{leu} -N _{cpa}]	1633.69	1633.96

Table 4. Binding affinity to CypA measured by fluorescence anisotropy.

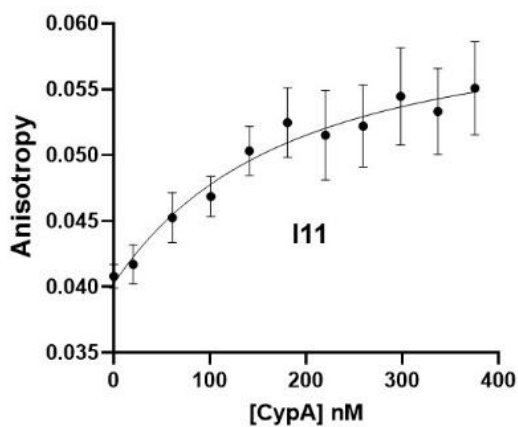
Compound	K_D (nM)
CsA	80.7 (\pm 15.0)
H11	399 (\pm 56)
H17	178 (\pm 36)
I11	153 (\pm 28)
I15	89.2 (\pm 8.7)

* All experimental data are shown as mean \pm SD (n=3).

Figure 18. Fluorescence anisotropy binding curves for CsA-CypA and I11-CypA interaction.



* The data points represent mean \pm SD (n=3).



* The data points represent mean \pm SD (n=3).

Optimization

To exert equipotent CypA inhibition to CsA, represented by suppressed expression of IL-2, 4,000 times higher concentration of the selected peptoids were needed. Even though the peptoids possess better properties such as lower cytotoxicity or better solubility, the optimization of the peptoids was required. I11, which showed most potent anti-inflammatory activity among the peptoids, was selected for the optimization. Since peptoids are poly N-substituted glycines, replacement of each peptoid monomer with glycines would show the contribution of each monomer to the binding to CypA (Fig. 19). Among five monomers, when the Npip was substituted with glycine, I11 lost the least CypA inhibiting activity, which showed the smallest contribution of Npip to the binding (Fig. 20). While Npip-to-Nleu substitution of I11 lost most of its IL-2 inhibition, replacement with bulkier Nnaph or Ndpe showed four times improvement of the IL-2 inhibition activity of I11 at 10 μ M. (Fig. 21 - 23). Still, one thousand times higher concentration of I11Ndpe was needed to show equipotent CypA inhibition to CsA. It seemed like this gap of efficiency cannot be narrowed easily even with further optimization. Therefore, I decided to focus on the monitoring of CypD inhibiting potency of the peptoids.

Figure 19. Glycine scanning of peptoid I11.

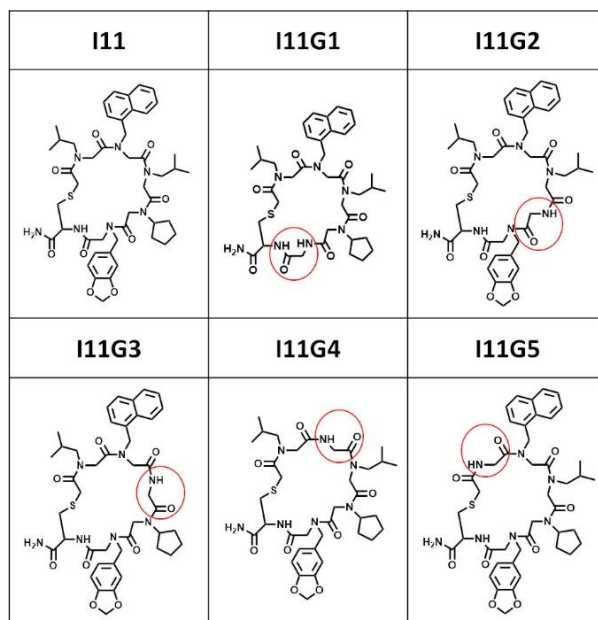
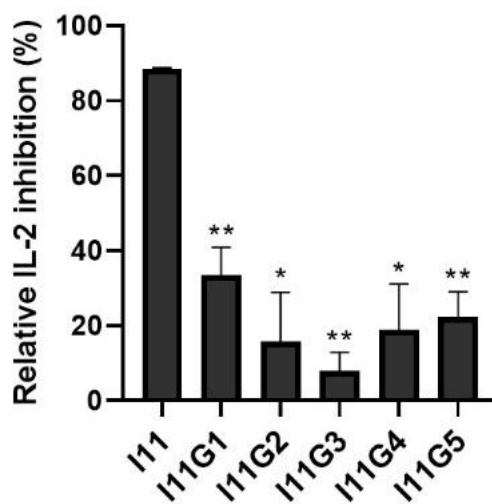


Figure 20. IL-2 inhibition of glycine scanning mutants of I11.



* All data are shown as mean \pm SD (n=2); *P \leq 0.05; **P \leq 0.01; Unpaired Student's t-test was performed compared to I11 using GraphPad Prism 8.

Figure 21. Modification of peptoid I11.

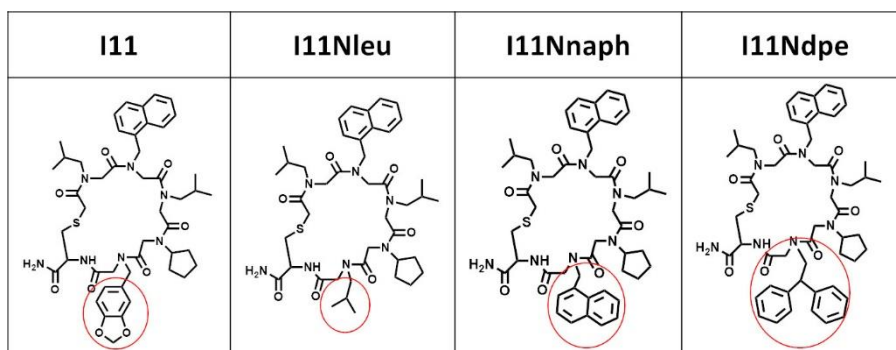
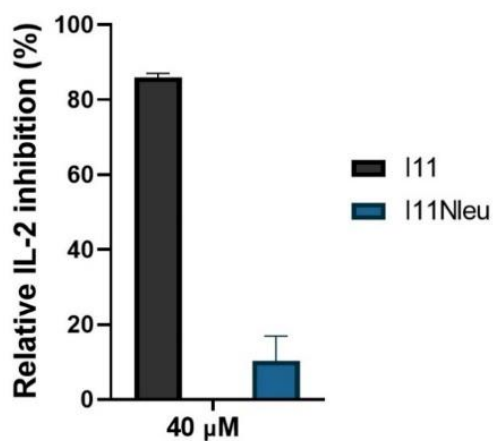
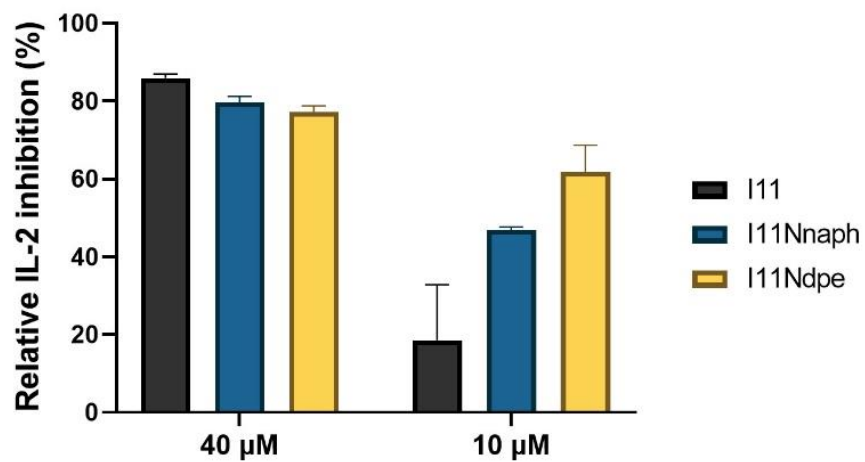


Figure 22. Loss of IL-2 inhibition of Npip-to-Nleu substitution of I11.



* All data are shown as mean \pm SD (n=2).

Figure 23. Improved IL-2 inhibition of modified I11.



* All data are shown as mean \pm SD (n=2).

Binding affinity of peptoids to CypD

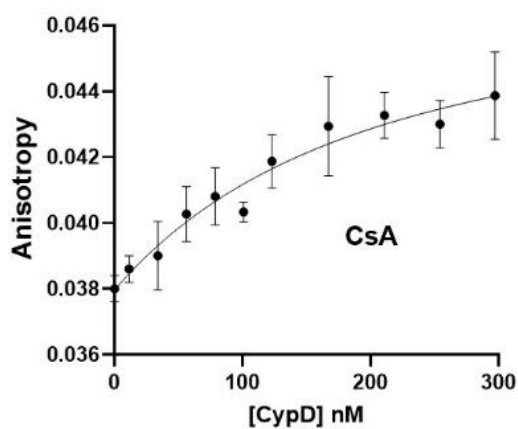
The binding affinities of cyclic peptoids to CypD were determined by fluorescence anisotropy method to select the effective CypD inhibitors. The results showed that I11 binds to CypD with $K_D = 619 \pm 96$ nM, while another peptoid, H17, binds to CypD with $K_D = 308 \pm 28$ nM (Table 5, Fig. 24). Even though the binding affinity of H17 to CypD is twofold stronger than that of I11, the anti-inflammatory activity of I11 is better than that of H17 at the same concentration.

Table 5. Binding affinity to CypD measured by fluorescence anisotropy.

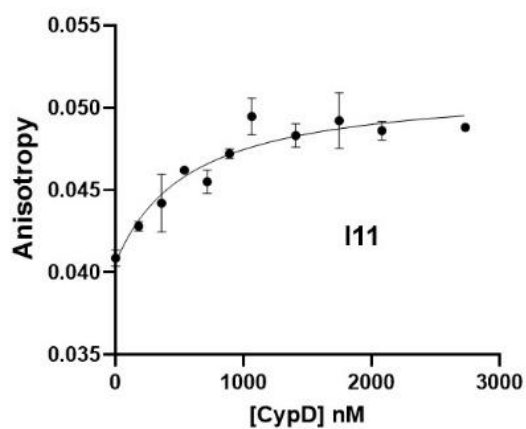
Compound	K_D (nM)
CsA	160 (± 28)
H11	846 (± 145)
H17	308 (± 27)
I11	619 (± 96)
I15	665 (± 60)

* All data are shown as mean \pm SD (n=3).

Figure 24. Fluorescence anisotropy binding curves for CsA-CypD and I11-CypD interaction.



* The data points represent mean \pm SD (n=3).



* The data points represent mean \pm SD (n=3).

Brain PAMPA

Brain permeability of neuroprotective agents is an important issue. Thus it is valuable to investigate blood-brain barrier (BBB) permeability of the compounds for CNS use. I tested passive permeability of the peptoids across BBB using parallel artificial membrane permeability assay (PAMPA) layered with porcine polar brain lipid extract (Table 6, Fig. 25).⁴⁸⁻⁵⁰ Peptoid I11 was shown to penetrate the BBB-mimic artificial membrane most efficiently, of which the effective permeability value, P_e , was calculated as $3.8 \times 10^{-6} \text{ cm s}^{-1}$, close to the high BBB permeation class (P_e ($10^{-6} \text{ cm s}^{-1}$) > 4.0) according to the previous report.⁵⁰ Verapamil was chosen as a high permeability standard ($P_e = 18 \times 10^{-6} \text{ cm s}^{-1}$), of which the result was almost same as the previously reported data.⁵⁰ Based on the results, I11 showed the most efficient BBB permeability followed by H17 and CsA in sequence. Therefore, peptoid I11 was chosen for further mitochondrial studies.

Figure 25. Concept of BBB-PAMPA.

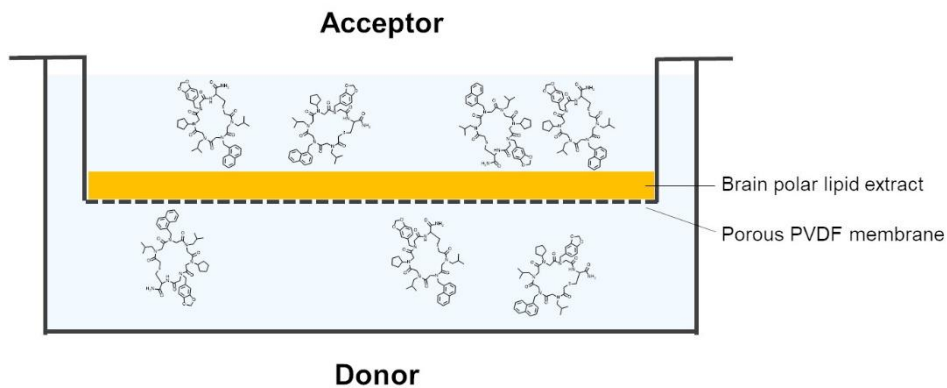


Table 6. Effective permeability (P_e) value from BBB-PAMPA.

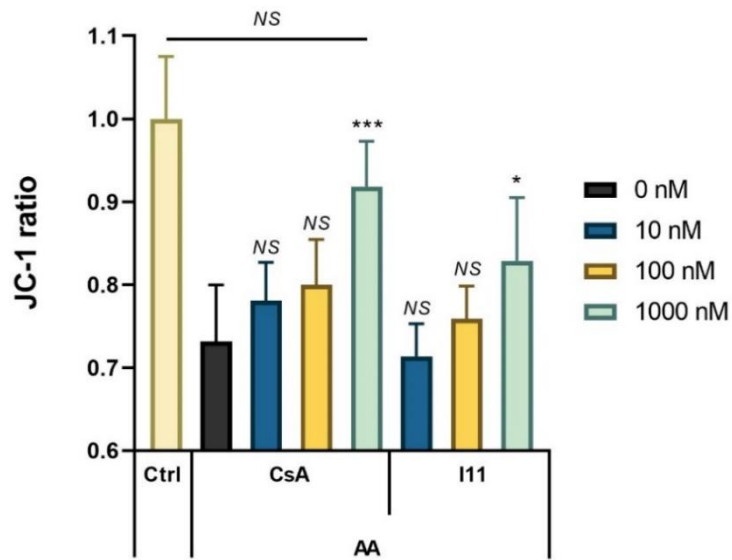
Compound	P_e (10^{-6} cm/s)
Verapamil	18 ± 6
CsA	1.7 ± 0.7
H17	2.9 ± 0.4
I11	3.8 ± 0.3

* All data are shown as mean \pm SD (n=3).

Mitochondrial membrane potential recovery effects in neuronal cell

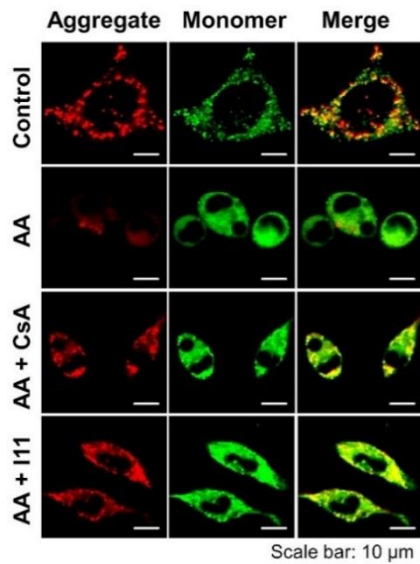
A variety of neuroprotective drugs have been investigated for restoring the mitochondria function. CsA is the most extensively studied drug by through the mechanism of inhibiting the opening of mitochondrial mPTP.^{34, 51} However, the physicochemical property of CsA inhibits its penetration of CNS barrier. As the most promising candidate for functional recovery of damaged mitochondria, mitochondrial membrane potential recovery effect of I11 was monitored by fluorescent JC-1 assay (Fig. 26 - 27). The mitochondrial function was examined in SH-SY5Y neuroblastoma cells using one of mitochondrial respiratory inhibitors, antimycin A. The JC-1 ratio, which represents the mitochondrial membrane potential ($\Delta\psi_m$), was decreased to 0.73 by the treatment of antimycin A at 20 μM . In the presence of CsA as positive control, dose-dependent increase was observed in the ratio. One μM of CsA increased the JC-1 ratio up to 0.91, which is not significantly different compared with the normal condition, while 1 μM of peptoid I11 recovered JC-1 ratio up to 0.83. This is prominent finding in that the binding affinity of peptoid I11 is four-fold weaker than that of CsA. In summary, these results showed that the depolarized mitochondrial membrane potential was recovered by the treatment of I11 as concentration-dependent manner.

Figure 26. Analysis of mitochondrial membrane potential in SH-SY5Y cells using JC-1 assay.



*All data are shown as mean \pm SD (n=3); *P \leq 0.05; ***P \leq 0.001; NS, not significant; Unpaired Student's t-test was performed compared to 0 nM using GraphPad Prism 8.

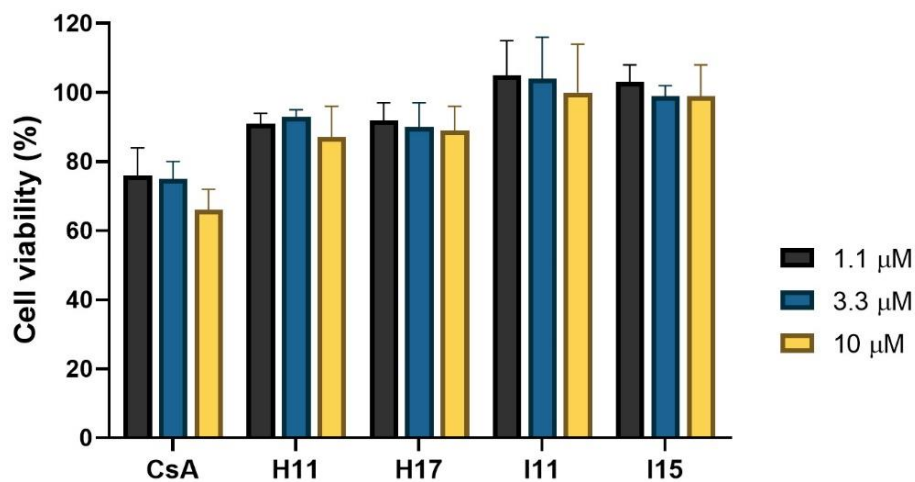
Figure 27. Monitoring of mitochondrial membrane potential in SH-SY5Y cells using CLSM.



Cytotoxicity

Cytotoxicity of the peptoids and CsA was examined in SH-SY5Y cells (Fig. 28). All the examined peptoids showed significantly better cell viability than CsA at the concentration of 1.1 μM , 3.3 μM and 10 μM . I11 showed no cytotoxicity up to 10 μM . Compared to CsA, I11 showed more than 20% higher cell viability at 1.1 μM , while the difference was bigger to 30% at 10 μM .

Figure 28. Effects of CsA and peptoids on viability of SH-SY5Y cells.



* All data are shown as mean \pm SD (n=4).

Biodistribution

To monitor biodistribution of I11, Cy5.5-labeled I11 was synthesized (Table 7, Fig. 29). Biodistribution of Cy5.5-labeled I11 was determined using IVIS Spectrum CT. Intense Cy5.5 signal was observed near the brain 30, 60, 90 and 230 min post-injection (Fig. 30 a). According to ex vivo imaging results, 4% of Cy5.5-I11 was distributed in brain (Fig. 30 b - c). Although it is difficult to confirm the BBB permeable property of I11 with this result as there was no consideration of organ weights or other compounds to be compared, this could support the PAMPA result where I11 showed quite a high BBB permeability.

Figure 29. Chromatogram of Cy5.5-I11.

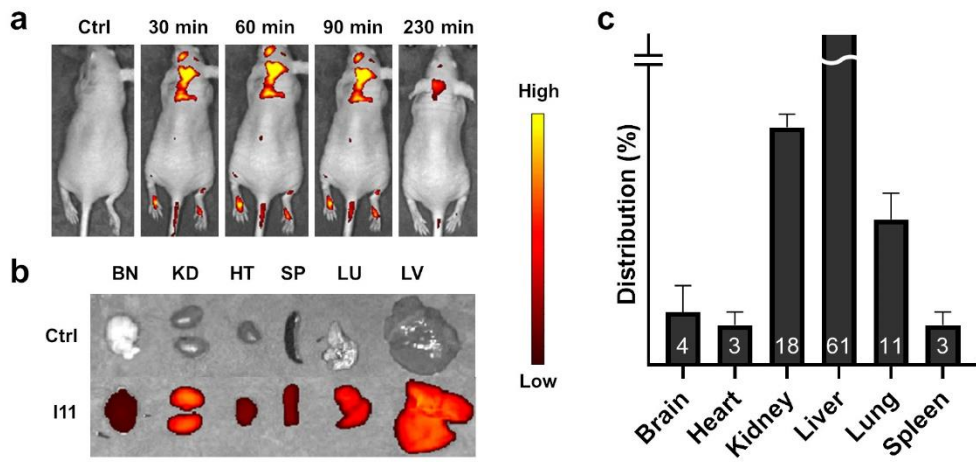
Cy5.5-I11 was obtained as a blue powder. The HPLC chromatogram of Cy5.5-I11 is shown below (95% purity).



Table 7. Sequence and mass data of Cy5.5-I11.

Peptoid	Sequence	MS [M+H] ⁺	
		Calcd.	Obsd.
Cy5.5-I11	Cy5.5-Lys-peg-cyclo[Cys-N _{pip} -N _{capa} -N _{leu} -N _{naph} -N _{leu}]	1738.92	1738.76

Figure 30. Biodistribution of Cy5.5-I11 measured by IVIS Spectrum CT.



* b) BN: brain; KD: kidney; HT: heart; SP: Spleen; LU: Lung; LV: Liver; c) All data are shown as mean \pm SD (n=3).

Conclusion

Cyclophilins (Cyps) were discovered more than 30 years ago but even today, the proteins are widely studied. It is maybe because of the accumulated body of data that human Cyps play critical roles in various human diseases. While the studies specify the roles of Cyps, there arise better understandings of the proteins, which in turn, produced more therapeutic targets to study. As previous studies showed the involvement of CypA in viral infection and replication, recent studies tried to apply the CypA inhibitors to severe acute respiratory syndrome coronavirus 2 (SARS-CoV-2), the virus causing the global pandemic, Coronavirus disease 19 (COVID-19).⁵²
⁵³ To my knowledge, this is the first study that identified cyclic peptoid Cyp inhibitors using OBOC library. The experimental design of this study was to identify Cyp inhibitors by OBOC library screening against the representative isoform, CypA. Binding affinity to CypA and IL-2 inhibition of the cyclic peptoids were correlated, but somehow the biological effect was not enough for CypA, which can be attributed to small binding surface or low binding specificity of cyclic penta-peptoids to CypA. However, the small size of these peptoids is not always disadvantageous in that the small size as well as appropriate lipophilicity contributes to better BBB permeability, an important issue when targeting CNS diseases. According to the results, cyclic peptoid I11 and H17 showed better BBB permeability and less cytotoxicity compared to CsA. Particularly, I11 showed equipotent mitochondrial membrane potential recovery to CsA. In conclusion, using OBOC cyclic peptoid library, I identified a novel CypD inhibitor I11 as a potential CNS disease-targeting agent.

Reference

1. Wang, P.; Heitman, J., The cyclophilins. *Genome Biol* **2005**, *6* (7), 226.
2. Nigro, P.; Pompilio, G.; Capogrossi, M. C., Cyclophilin A: a key player for human disease. *Cell Death Dis* **2013**, *4*, e888.
3. Obchoei, S.; Wongkhan, S.; Wongkham, C.; Li, M.; Yao, Q.; Chen, C., Cyclophilin A: potential functions and therapeutic target for human cancer. *Med Sci Monit* **2009**, *15* (11), RA221-32.
4. Watashi, K.; Shimotohno, K., Cyclophilin and viruses: cyclophilin as a cofactor for viral infection and possible anti-viral target. *Drug Target Insights* **2007**, *2*, 9-18.
5. Du, H.; Guo, L.; Fang, F.; Chen, D.; Sosunov, A. A.; McKhann, G. M.; Yan, Y.; Wang, C.; Zhang, H.; Molkenstin, J. D.; Gunn-Moore, F. J.; Vonsattel, J. P.; Arancio, O.; Chen, J. X.; Yan, S. D., Cyclophilin D deficiency attenuates mitochondrial and neuronal perturbation and ameliorates learning and memory in Alzheimer's disease. *Nat Med* **2008**, *14* (10), 1097-105.
6. Saphire, A. C.; Bobardt, M. D.; Galloway, P. A., Human immunodeficiency virus type 1 hijacks host cyclophilin A for its attachment to target cells. *Immunol Res* **2000**, *21* (2-3), 211-7.
7. Davis, T. L.; Walker, J. R.; Campagna-Slater, V.; Finerty, P. J.; Paramanathan, R.; Bernstein, G.; MacKenzie, F.; Tempel, W.; Hui, O. Y.; Lee, W. H.; Eisenmesser, E. Z.; Dhe-Paganon, S., Structural and Biochemical Characterization of the Human Cyclophilin Family of Peptidyl-Prolyl Isomerases. *Plos Biol* **2010**, *8* (7).
8. Galat, A.; Metcalfe, S. M., Peptidylproline Cis/Trans Isomerases. *Prog Biophys Mol Bio* **1995**, *63* (1), 67-118.
9. Handschumacher, R. E.; Harding, M. W.; Rice, J.; Drugge, R. J.; Speicher,

- D. W., Cyclophilin: a specific cytosolic binding protein for cyclosporin A. *Science* **1984**, 226 (4674), 544-7.
10. Suzuki, J.; Jin, Z. G.; Meoli, D. F.; Matoba, T.; Berk, B. C., Cyclophilin A is secreted by a vesicular pathway in vascular smooth muscle cells. *Circ Res* **2006**, 98 (6), 811-817.
 11. Sherry, B.; Yarlett, N.; Strupp, A.; Cerami, A., Identification of Cyclophilin as a Proinflammatory Secretory Product of Lipopolysaccharide-Activated Macrophages. *P Natl Acad Sci USA* **1992**, 89 (8), 3511-3515.
 12. Jin, Z. G.; Melaragno, M. G.; Liao, D. F.; Yan, C.; Haendeler, J.; Suh, Y. A.; Lambeth, J. D.; Berk, B. C., Cyclophilin A is a secreted growth factor induced by oxidative stress. *Circ Res* **2000**, 87 (9), 789-796.
 13. Clipstone, N. A.; Crabtree, G. R., Identification of calcineurin as a key signalling enzyme in T-lymphocyte activation. *Nature* **1992**, 357 (6380), 695-7.
 14. Liu, J.; Farmer, J. D., Jr.; Lane, W. S.; Friedman, J.; Weissman, I.; Schreiber, S. L., Calcineurin is a common target of cyclophilin-cyclosporin A and FKBP-FK506 complexes. *Cell* **1991**, 66 (4), 807-15.
 15. Porter, G. A.; Beutner, G., Cyclophilin D, Somehow a Master Regulator of Mitochondrial Function. *Biomolecules* **2018**, 8 (4).
 16. Javadov, S.; Kuznetsov, A., Mitochondrial permeability transition and cell death: the role of cyclophilin D. *Front Physiol* **2013**, 4.
 17. Giorgio, V.; Soriano, M. E.; Basso, E.; Bisetto, E.; Lippe, G.; Forte, M. A.; Bernardi, P., Cyclophilin D in mitochondrial pathophysiology. *Bba-Bioenergetics* **2010**, 1797 (6-7), 1113-1118.
 18. Kinnally, K. W.; Peixoto, P. M.; Ryu, S. Y.; Dejean, L. M., Is mPTP the gatekeeper for necrosis, apoptosis, or both? *Bba-Mol Cell Res* **2011**, 1813 (4), 616-622.

19. Du, H.; Guo, L.; Fang, F.; Chen, D.; Sosunov, A. A.; McKhann, G. M.; Yan, Y. L.; Wang, C. Y.; Zhang, H.; Molkentin, J. D.; Gunn-Moore, F. J.; Vonsattel, J. P.; Arancio, O.; Chen, J. X.; Du Yan, S., Cyclophilin D deficiency attenuates mitochondrial and neuronal perturbation and ameliorates learning and memory in Alzheimer's disease. *Nature Medicine* **2008**, *14* (10), 1097-1105.
20. Sun, J. L.; Jacobs, K. M., Knockout of Cyclophilin-D Provides Partial Amelioration of Intrinsic and Synaptic Properties Altered by Mild Traumatic Brain Injury. *Front Syst Neurosci* **2016**, *10*.
21. Gainutdinov, T.; Molkentin, J. D.; Siemen, D.; Ziemer, M.; Debska-Vielhaber, G.; Vielhaber, S.; Gizatullina, Z.; Orynbayeva, Z.; Gellerich, F. N., Knockout of cyclophilin D in Ppif(-/-) mice increases stability of brain mitochondria against Ca²⁺ stress. *Archives of Biochemistry and Biophysics* **2015**, *579*, 40-46.
22. Calne, R. Y.; Pentlow, B. D.; White, D. J. G.; Evans, D. B.; McMaster, P.; Rolles, K.; Dunn, D. C.; Thiru, S.; Craddock, G. N., Cyclosporin-a in Patients Receiving Renal-Allografts from Cadaver Donors. *Lancet* **1978**, *2* (8104), 1323-1327.
23. Colgan, J.; Asmal, M.; Yu, B.; Luban, J., Cyclophilin A-deficient mice are resistant to immunosuppression by cyclosporine. *J Immunol* **2005**, *174* (10), 6030-8.
24. Bennett, W. M.; Norman, D. J., Action and toxicity of cyclosporine. *Annu Rev Med* **1986**, *37*, 215-24.
25. Busauschina, A.; Schnuelle, P.; van der Woude, F. J., Cyclosporine nephrotoxicity. *Transplant P* **2004**, *36* (2), 229s-233s.
26. Pardridge, W. M., Blood-brain barrier delivery. *Drug Discov Today* **2007**, *12* (1-2), 54-61.

27. Tsuji, A.; Tamai, I.; Sakata, A.; Tenda, Y.; Terasaki, T., Restricted transport of cyclosporin A across the blood-brain barrier by a multidrug transporter, P-glycoprotein. *Biochem Pharmacol* **1993**, *46* (6), 1096-9.
28. Kirkinezos, I. G.; Hernandez, D.; Bradley, W. G.; Moraes, C. T., An ALS mouse model with a permeable blood-brain barrier benefits from systemic cyclosporine A treatment. *J Neurochem* **2004**, *88* (4), 821-826.
29. Waldmeier, P. C.; Feldtrauer, J. J.; Qian, T.; Lemasters, J. J., Inhibition of the mitochondrial permeability transition by the nonimmunosuppressive cyclosporin derivative NIM811. *Mol Pharmacol* **2002**, *62* (1), 22-9.
30. Hansson, M. J.; Mattiasson, G.; Mansson, R.; Karlsson, J.; Keep, M. F.; Waldmeier, P.; Ruegg, U. T.; Dumont, J. M.; Besseghir, K.; Elmer, E., The nonimmunosuppressive cyclosporin analogs NIM811 and UNIL025 display nanomolar potencies on permeability transition in brain-derived mitochondria. *J Bioenerg Biomembr* **2004**, *36* (4), 407-13.
31. Sakamoto, K.; Tsuji, E.; Miyauchi, M.; Nakanishi, T.; Yamashita, M.; Shigematsu, N.; Tada, T.; Izumi, S.; Okuhara, M., Fr901459, a Novel Immunosuppressant Isolated from *Stachybotrys Chartarum* No 19392 - Taxonomy of the Producing Organism, Fermentation, Isolation, Physicochemical Properties and Biological-Activities (Vol 46, Pg 1788, 1993). *J Antibiot* **1994**, *47* (2), C1-C1.
32. Murphy, M. P., Targeting lipophilic cations to mitochondria. *Biochim Biophys Acta* **2008**, *1777* (7-8), 1028-31.
33. Malouitre, S.; Dube, H.; Selwood, D.; Crompton, M., Mitochondrial targeting of cyclosporin A enables selective inhibition of cyclophilin-D and enhanced cytoprotection after glucose and oxygen deprivation. *Biochem J* **2009**, *425* (1), 137-48.
34. Warne, J.; Pryce, G.; Hill, J. M.; Shi, X.; Lenneras, F.; Puentes, F.;

- Kip, M.; Hilditch, L.; Walker, P.; Simone, M. I.; Chan, A. W.; Towers, G. J.; Coker, A. R.; Duchon, M. R.; Szabadkai, G.; Baker, D.; Selwood, D. L., Selective Inhibition of the Mitochondrial Permeability Transition Pore Protects against Neurodegeneration in Experimental Multiple Sclerosis. *J Biol Chem* **2016**, *291* (9), 4356-73.
35. Gradler, U.; Schwarz, D.; Blaesse, M.; Leuthner, B.; Johnson, T. L.; Bernard, F.; Jiang, X. L.; Marx, A.; Gilardone, M.; Lemoine, H.; Roche, D.; Jorand-Lebrun, C., Discovery of novel Cyclophilin D inhibitors starting from three dimensional fragments with millimolar potencies. *Bioorganic & Medicinal Chemistry Letters* **2019**, *29* (23).
36. Ahmed-Belkacem, A.; Colliandre, L.; Ahnou, N.; Nevers, Q.; Gelin, M.; Bessin, Y.; Brillet, R.; Cala, O.; Douguet, D.; Bourguet, W.; Krimm, I.; Pawlotsky, J. M.; Guichou, J. F., Fragment-based discovery of a new family of non-peptidic small-molecule cyclophilin inhibitors with potent antiviral activities. *Nat Commun* **2016**, *7*, 12777.
37. Guichou, J. F.; Viaud, J.; Mettling, C.; Subra, G.; Lin, Y. L.; Chavanieu, A., Structure-based design, synthesis, and biological evaluation of novel inhibitors of human cyclophilin A. *J Med Chem* **2006**, *49* (3), 900-10.
38. Ni, S.; Yuan, Y.; Huang, J.; Mao, X.; Lv, M.; Zhu, J.; Shen, X.; Pei, J.; Lai, L.; Jiang, H.; Li, J., Discovering potent small molecule inhibitors of cyclophilin A using de novo drug design approach. *J Med Chem* **2009**, *52* (17), 5295-8.
39. Kwon, Y. U.; Kodadek, T., Quantitative evaluation of the relative cell permeability of peptoids and peptides. *J Am Chem Soc* **2007**, *129* (6), 1508-9.
40. Miller, S. M.; Simon, R. J.; Ng, S.; Zuckermann, R. N.; Kerr, J. M.; Moos, W. H., Comparison of the Proteolytic Susceptibilities of Homologous L-Amino-Acid, D-Amino-Acid, and N-Substituted Glycine Peptide and Peptoid Oligomers.

Drug Develop Res **1995**, 35 (1), 20-32.

41. Schwochert, J.; Turner, R.; Thang, M.; Berkeley, R. F.; Ponkey, A. R.; Rodriguez, K. M.; Leung, S. S. F.; Khunte, B.; Goetz, G.; Limberakis, C.; Kalgutkar, A. S.; Eng, H.; Shapiro, M. J.; Mathiowetz, A. M.; Price, D. A.; Liras, S.; Jacobson, M. P.; Lokey, R. S., Peptide to Peptoid Substitutions Increase Cell Permeability in Cyclic Hexapeptides. *Organic Letters* **2015**, 17 (12), 2928-2931.
42. Shin, M. K.; Hyun, Y. J.; Lee, J. H.; Lim, H. S., Comparison of Cell Permeability of Cyclic Peptoids and Linear Peptoids. *Acs Combinatorial Science* **2018**, 20 (4), 237-242.
43. Beekman, N. J.; Schaaper, W. M.; Tesser, G. I.; Dalsgaard, K.; Kamstrup, S.; Langeveld, J. P.; Boshuizen, R. S.; Meloen, R. H., Synthetic peptide vaccines: palmitoylation of peptide antigens by a thioester bond increases immunogenicity. *J Pept Res* **1997**, 50 (5), 357-64.
44. Shin, M. H.; Lee, K. J.; Lim, H.-S., DNA-Encoded Combinatorial Library of Macrocyclic Peptoids. *Bioconjugate Chemistry* **2019**, 30 (11), 2931-2938.
45. Liu, T.; Qian, Z.; Xiao, Q.; Pei, D., High-Throughput Screening of One-Bead-One-Compound Libraries: Identification of Cyclic Peptidyl Inhibitors against Calcineurin/NFAT Interaction. *ACS Combinatorial Science* **2011**, 13 (5), 537-546.
46. Ke, H.; Mayrose, D.; Belshaw, P. J.; Alberg, D. G.; Schreiber, S. L.; Chang, Z. Y.; Etkorn, F. A.; Ho, S.; Walsh, C. T., Crystal structures of cyclophilin A complexed with cyclosporin A and N-methyl-4-[(E)-2-butenyl]-4,4-dimethylthreonine cyclosporin A. *Structure* **1994**, 2 (1), 33-44.
47. Husi, H.; Zurini, M. G. M., Comparative Binding Studies of Cyclophilins to Cyclosporine A and Derivatives by Fluorescence Measurements. *Analytical Biochemistry* **1994**, 222 (1), 251-255.

48. Bicker, J.; Alves, G.; Fortuna, A.; Soares-da-Silva, P.; Falcão, A., A new PAMPA model using an in-house brain lipid extract for screening the blood–brain barrier permeability of drug candidates. *International Journal of Pharmaceutics* **2016**, *501* (1), 102-111.
49. Di, L.; Kerns, E. H.; Bezar, I. F.; Petusky, S. L.; Huang, Y., Comparison of blood–brain barrier permeability assays: in situ brain perfusion, MDR1-MDCKII and PAMPA-BBB. *Journal of Pharmaceutical Sciences* **2009**, *98* (6), 1980-1991.
50. Di, L.; Kerns, E. H.; Fan, K.; McConnell, O. J.; Carter, G. T., High throughput artificial membrane permeability assay for blood–brain barrier. *European journal of medicinal chemistry* **2003**, *38* (3), 223-232.
51. Rao, V. K.; Carlson, E. A.; Yan, S. S., Mitochondrial permeability transition pore is a potential drug target for neurodegeneration. *Biochimica et Biophysica Acta (BBA) - Molecular Basis of Disease* **2014**, *1842* (8), 1267-1272.
52. Softic, L.; Brillet, R.; Berry, F.; Ahnou, N.; Nevers, Q.; Morin-Dewaele, M.; Hamadat, S.; Bruscella, P.; Fourati, S.; Pawlotsky, J. M.; Ahmed-Belkacem, A., Inhibition of SARS-CoV-2 Infection by the Cyclophilin Inhibitor Alisporivir (Debio 025). *Antimicrob Agents Chemother* **2020**, *64* (7).
53. Liu, C.; von Brunn, A.; Zhu, D., Cyclophilin A and CD147: novel therapeutic targets for the treatment of COVID-19. *Med Drug Discov* **2020**, *7*, 100056.

국문초록

Cyclophilin (Cyp) 은 펩타이드 프롤린의 시스-트랜스 이성질화에 관여하는 효소이다. 인간에게는 서열이 유사한 17 개의 Cyp 동형 단백질이 있는데, 그 중 가장 많이 발견되어 있고 가장 먼저 발견된 것은 cyclophilin A (CypA) 이다. CypA 는 주로 세포질에 위치하며 류마티스 관절염, 알츠하이머 병, 암 및 바이러스 감염과 같은 많은 인간 질병에 관여하고 있다. 최근에는 코로나바이러스감염증-19에 의한 팬데믹 상황을 가져온 바이러스인 SARS-CoV-2 에 Cyp 저해제를 적용하려는 연구도 이루어지고 있다. 또 다른 동형 단백질인 cyclophilin D (CypD) 는 미토콘드리아의 기질에 위치하며, Ca^{2+} 에 의해 유도되는 미토콘드리아 투과성 전이 기공 (mPTP, Mitochondrial permeability transition pore) 의 개방에 중요한 역할을 하는 것으로 알려져 있다. 미토콘드리아 투과성 전이 기공이 열리면, cytochrome C 가 세포질로 방출되며 세포사멸을 유도하여 여러가지 질병을 일으킬 수 있다.

한편, cyclosporine A (CsA) 는 Cyp 의 천연 억제제로, 적은 농도로 사이클로필린 활성을 억제한다. 그러나 CsA 는 독성이 높은 편이고 용해도가 낮아서 약으로 쓰이기 어려운 특징을 가지며, 뇌혈관장벽을 잘 통과하지 못해서 중추신경계 약물로 사용하기 어렵다. 따라서 CsA 를 이용할 수 있는 새로운 전략이나, 비슷한 효과를 내는 새로운 화합물의 개

발이 필요하다.

이 연구에서는 OBOC (One-bead-one-compound) 고리형 펩타이드 라이브러리를 이용하여 CypA 에 잘 결합하는 물질들을 얻고, 여러가지 실험을 통해 새로운 Cyp 억제제를 발굴하고자 하였다. 고리형 펩타이드 I11 은 CsA 와 비슷한 수준의 미토콘드리아 막 전위 회복 능력을 보이면서, 세포 독성은 더 낮고 뇌혈관장벽에 대한 투과성은 더 좋을 것으로 나타났다. 따라서 이 연구에서는 고리형 펩타이드 라이브러리의 구축 및 스크리닝을 통해, 고리형 펩타이드가 가지는 장점을 이용하여, CypD 가 관여하는 중추신경계 질환에 기존의 CsA 보다 더 적합한 물질을 발굴해 내었다는 의의가 있다.

키워드: cyclophilin A, cyclophilin D, one-bead-one-compound, 라이브러리 스크리닝, 펩타이드, 펩타이드 유사체, 미토콘드리아 투과성 전이 기공, 뇌혈관장벽

학번: 2018-22030